

Health benefits attributed to 17 α -estradiol, a lifespan-extending compound, are mediated through estrogen receptor α

Shivani N. Mann^{1,2,3}, Niran Hadad⁴, Molly Nelson-Holte⁵, Alicia R. Rothman¹, Roshini Sathiaseelan¹, Samim Ali-Mondal¹, Martin-Paul Agbaga^{3,6,7}, Archana Unnikrishnan^{3,8}, Malayannan Subramaniam⁵, John Hawse⁵, Derek M. Huffman⁹, Willard M. Freeman^{2,10,11}, Michael B. Stout^{1,2,3}

Institutions:

¹Department of Nutritional Sciences, University of Oklahoma Health Sciences Center, Oklahoma City, OK

²Oklahoma Center for Geroscience, University of Oklahoma Health Sciences Center, Oklahoma City, OK

³Harold Hamm Diabetes Center, University of Oklahoma Health Sciences Center, Oklahoma City, OK

⁴The Jackson Laboratory, Bar Harbor, ME

⁵Department of Biochemistry and Molecular Biology, Mayo Clinic, Rochester, MN

⁶Department of Cell Biology, University of Oklahoma Health Sciences Center, Oklahoma City, OK

⁷Dean McGee Eye Institute, University of Oklahoma Health Sciences Center, Oklahoma City, OK

⁸Department of Biochemistry and Molecular Biology, University of Oklahoma Health Sciences Center, Oklahoma City, OK

⁹Department of Molecular Pharmacology, Albert Einstein College of Medicine, New York, NY

¹⁰Genes & Human Disease Research Program, Oklahoma Medical Research Foundation, Oklahoma City, OK

¹¹Oklahoma City Veterans Affairs Medical Center, Oklahoma City, OK

Correspondence To:

Michael B. Stout

1200 N Stonewall Ave, Suite 3057

University of Oklahoma Health Sciences Center

Oklahoma City, OK 73117

Phone: 405-271-2113

Fax: 405-271-1560

michael-stout@ouhsc.edu

Email Addresses of Authors:

Shivani N. Mann shivani-mann@ouhsc.edu

Niran Hadad Niran.Hadad@jax.org

Molly Nelson-Holte NelsonHolte.Molly@mayo.edu

Alicia R. Rothman Alicia-rothman@ouhsc.edu

Roshini Sathiaseelan Roshini-sathiaseelan@ouhsc.edu

Samim Ali-Mondal Samim-alimondal@ouhsc.edu

Martin-Paul Agbaga martin-paul-agbaga@ouhsc.edu

Archana Unnikrishnan Archana-Unnikrishnan@ouhsc.edu

Subramaniam Malayannan Subramaniam.Malayannan@mayo.edu

John Hawse Hawse.John@mayo.edu

Derek M. Huffman derek.huffman@einstein.yu.edu

Willard M. Freeman bill-freeman@omrf.org

ABSTRACT

Metabolic dysfunction underlies several chronic diseases, many of which are exacerbated by obesity. Dietary interventions can reverse metabolic declines and slow aging, although compliance issues remain paramount. 17 α -estradiol treatment improves metabolic parameters and slows aging in male mice. The mechanisms by which 17 α -estradiol elicits these benefits remain unresolved. Herein, we show that 17 α -estradiol elicits similar genomic binding and transcriptional activation through estrogen receptor α (ER α) to that of 17 β -estradiol. In addition, we show that the ablation of ER α completely attenuates the beneficial metabolic effects of 17 α -E2 in male mice. Our findings suggest that 17 α -E2 acts primarily through the liver and hypothalamus to improve metabolic parameters in male mice. Lastly, we also determined that 17 α -E2 improves metabolic parameters in male rats, thereby proving that the beneficial effects of 17 α -E2 are not limited to mice. Collectively, these studies suggest ER α may be a drug target for mitigating chronic diseases in male mammals.

KEYWORDS

17 α -estradiol, aging, estrogen receptor, hypothalamus, liver, metabolism, obesity

INTRODUCTION

Aging is the leading risk factor for most chronic diseases, many of which are associated with declines in metabolic homeostasis [1]. Metabolic detriments associated with advancing age are further exacerbated by obesity [2, 3], which has risen substantially in the older population (> 65 years) over the past several decades [4, 5]. Moreover, obesity in mid-life has been shown to accelerate aging mechanisms and induce phenotypes more commonly observed in older mammals [6-12]. These observations have led many to postulate that obesity may represent a mild progeria syndrome [13-17]. Although it is well established that dietary interventions, including calorie restriction, can reverse obesity-related metabolic sequelae, many of these strategies are not well-tolerated in older patients due to concomitant comorbidities [2, 18]. Compliance issues across all age groups also remain a paramount hurdle due to calorie restriction adversely affecting mood, thermoregulation, and musculoskeletal mass [19]. These adverse health outcomes demonstrate the need for pharmacological approaches aimed at curtailing metabolic perturbations associated with obesity and aging.

17 α -estradiol (17 α -E2) is one of the more recently studied compounds to demonstrate efficacy for beneficially modulating obesity- and age-related health outcomes. The NIA Interventions Testing Program (ITP) found that long-term administration of 17 α -E2 extends median lifespan of male mice in a dose-dependent manner [20, 21]. Our group has been exploring potential mechanisms by which 17 α -E2 may improve healthspan and extend lifespan in a sex-specific manner. We have found that 17 α -E2 administration reduces calorie intake and regional adiposity in combination with significant improvements in a multitude of systemic metabolic parameters in both middle-aged obese and old male mice without inducing deleterious effects [22-24]. Other groups have also determined that lifelong administration of 17 α -E2 beneficially modulates metabolic outcomes, including glucose tolerance, mTORC2 signaling, and hepatic amino acid composition and markers of urea cycling, which were reported to be dependent upon the presence of endogenous androgens [25, 26]. Additionally, multiple lifespan extending compounds, including 17 α -E2, exhibit similar modifications in liver function [27]. In all, recent studies by several independent laboratories strongly indicate that the lifespan-extending effects of 17 α -E2 are at least associated with, if not dependent on, metabolic improvements.

Despite the mounting evidence demonstrating that 17 α -E2 improves numerous health parameters, the signaling mechanism(s) and primary tissues through which 17 α -E2 elicits these benefits remain unknown. Although 17 α -E2 is a naturally-occurring enantiomer to 17 β -estradiol (17 β -E2), it has been postulated that 17 α -E2 signals through a novel uncharacterized receptor [28-31] as opposed to classical estrogen receptors α (ER α) and β (ER β); which is due to 17 α -E2 having significantly reduced binding affinity for ER α and ER β as compared to 17 β -E2 [32-35]. For this reason, 17 α -E2 is often referred to as a non-feminizing estrogen [31, 36, 37]. A few studies have suggested that a novel estrogen receptor, termed ER-X, may mediate 17 α -E2 actions in the brain [28-31], although more recent studies supporting this hypothesis are lacking in the literature. Similarly, no reports to date have directly tested whether the doses of 17 α -E2 shown to improve healthspan and lifespan in mice are mediated through ER α and/or ER β .

There is a multitude of data in the diabetes and metabolism literature demonstrating that ER α plays a major role in regulating systemic metabolic parameters. Although most of these studies have historically been performed in female mammals, more recent studies have demonstrated that ER α also plays a critical role in modulating metabolism in male mammals. For instance, Allard and colleagues recently demonstrated that genomic actions of ER α regulate systemic glucose homeostasis in mice of both sexes and insulin production and release in males [38]. Other studies have also determined that hepatic steatosis and insulin sensitivity, and therefore the control of gluconeogenesis, are regulated through FOXO1 in an ER α -dependent manner in male mice [39]. Furthermore, hepatocyte-specific deletion of ER α was sufficient to abrogate similar estrogen-mediated metabolic benefits [40-42]. Given that several reports have linked the administration of 17 α -E2 to improvements in metabolic homeostasis, we hypothesized that 17 α -E2 signals through ER α to modulate hepatic function and systemic metabolism, thereby potentially contributing to the lifespan-extending effects of 17 α -E2.

The work outlined in this report sought to determine if ER α is the primary receptor by 17 α -E2 modulates health parameters. As described above, ER α plays a major role in regulating hepatic function and systemic metabolism, both of which are improved with 17 α -E2 treatment. However, no studies to date have tested this potential connection *in vivo*. In this study, we treated obese wild type (WT) and ER α global knockout (ER α KO) littermate mice with 17 α -E2 to determine if the ablation of ER α could attenuate 17 α -E2-induced benefits on adiposity, metabolic homeostasis, and hepatic function. We found that the ablation of ER α completely attenuated all beneficial metabolic effects of 17 α -E2 in male mice, and no effects of 17 α -E2 were observed in female mice of either genotype. Follow-up studies in male WT rats undergoing hyperinsulinemic-euglycemic clamps revealed that 17 α -E2 modulates hepatic insulin sensitivity following acute exposure. Given the established connection between the hypothalamus and liver in the modulation of hepatic insulin sensitivity [43-47], coupled with our data demonstrating ER α -dependency of 17 α -E2 actions on metabolic parameters, we speculate that 17 α -E2 acts through ER α in the liver and/or hypothalamus to improve metabolic homeostasis in male mammals.

RESULTS

17 α -E2 and 17 β -E2 similarly modulate transcriptional activity of ER α

It is well established that ligand-mediated ER α dimerization leads to nuclear translocation and transcriptional activity. Previous work has shown that 17 α -E2 and 17 β -E2 can bind to ER α with different affinities [32-35], yet potential differences in downstream transcriptional activity between the two ligands remains unexplored. To determine if 17 α -E2 and 17 β -E2 induce similar transcriptional activity through ER α , we assessed ER α DNA binding and transcriptional induction following exposure to 17 β -E2 (10nM) or 17 α -E2 (10nM or 100nM) in U2OS cells that stably-express ER α following doxycycline induction. We chose to use these cells because they do not endogenously express any form of ER α or ER β and have been extensively utilized to elucidate the effects of ER α and ER β agonists and antagonists on global gene expression profiles [48, 49]. We found that 17 α -E2 and 17 β -E2 induced nearly identical ER α DNA binding signatures (Figure 1A, Figure 1-figure supplement 1). Relative to vehicle treated cells, treatment with 10nM 17 α -E2 induced 14,939 ER α binding sites (FDR < 0.05),

100nM 17 α -E2 induced 19,563 ER α binding sites (FDR < 0.05), and 10nM 17 β -E2 induced 20,668 ER α binding sites (FDR < 0.05). However, no statistically significant difference in ER α binding was observed when comparing treatment groups across different ligands and ligand concentrations. As expected, ER α binding sites were enriched for estrogen response elements (ERE), estrogen-related receptor beta (ESRRB), and estrogen-related receptor alpha (ESRRA). Other common motifs found within ER elements, including steroidogenic factor-1 (SF-1) [50], and motif elements of known interacting partners, including retinoid acid receptor:retinoid X receptor (RAR:RXR) [51], were also enriched (Figure 1B). In addition, we observed enrichment of androgen response elements (ARE) in ER α peaks (Figure 1B). Of particular relevance, many of the top enriched motifs identified contained the ERE consensus sequence TTGAC, which is shown in Supplementary File 1. Furthermore, there were no differences in the binding motifs identified between treatment groups (Figure 1B).

Next, we examined potential differences in transcriptional responses between treatment groups using RNA-sequencing. Principle component analysis based on the entire transcriptome revealed that all samples exposed to either 17 α -E2 or 17 β -E2 clustered together, whereas vehicle treated cells remained distinctly separated from treated cells on the first principle component, which explains the majority of the variance in transcription (70.64%) (Figure 1C). These data suggest that treatment vs vehicle is the primary covariate explaining variance in transcriptional profiles. Whereas the type of treatment plays a minimal role in transcriptional differences. Next, differential expression was assessed between all groups using a negative binomial regression model. No genes were found to be differentially regulated (FDR < 0.05) between the estrogen treatments. Yet, compared to vehicle treated cells, treatment of U2OS cells with either 10nM or 100nM 17 α -E2 or 10nM 17 β -E2 resulted in nearly identical gene suppression and activation signatures (Figure 1D, left). Additionally, both 17 α -E2 or 17 β -E2 treatment conditions resulted in higher ER α DNA binding affinity to gene bodies of these differentially expressed transcripts compared to vehicle treatment, and no differences were observed between 17 α -E2 and 17 β -E2 conditions (Figure 1D, right). These findings led us to postulate that 17 α -E2 may be the signaling through ER α to modulate health parameters in male mice. As such, we subsequently sought to determine if the ablation of ER α *in vivo* would mitigate the effects of 17 α -E2.

ER α ablation attenuates 17 α -E2-mediated benefits on metabolic parameters in male mice *in vivo*

To induce obesity and metabolic perturbations in male mice, we administered high-fat diet (HFD) for several months prior to initiating 17 α -E2 treatment. Almost immediately after 17 α -E2 treatment began, male WT mice displayed significant reductions in mass (Figure 2A-B) and adiposity (Figure 2C-D). This is aligned with our previous reports demonstrating that 17 α -E2 administration quickly reduces body mass and adiposity [22-24], which we have linked to hypothalamic regulation of anorexigenic signaling pathways [23]. Indeed, male WT mice in the current study also displayed robust declines in calorie consumption during the first four weeks of treatment (Figure 2E). Conversely, all of these benefits were completely abolished in male mice lacking ER α (ER α KO),

thereby confirming that 17 α -E2 definitively acts through ER α to modulate feeding behaviors, mass, and adiposity in male mice. Given the close association between adiposity and metabolic homeostasis, coupled with our previous work demonstrating the ability of 17 α -E2 to improve metabolic parameters [22, 23], we also assessed several metabolic variables in these studies. Similar to the mass and adiposity data described above, male WT mice receiving 17 α -E2 displayed significant improvements in fasting insulin (Figure 3B), HbA1C (Figure 3C), and glucose tolerance (Figure 3D-E, Figure 3-figure supplement 1); whereas male ER α KO mice receiving 17 α -E2 failed to recapitulate these findings. Interestingly, despite the masses of the male WT 17 α -E2 treatment group being nearly 15 grams greater than those of the male WT chow-fed controls, glucose tolerance was essentially identical between these groups, thereby indicating that 17 α -E2 restores metabolic flexibility in the presence of obesity in male mice (Figure 3D-E, Figure 3-figure supplement 1). We also evaluated the effects of 17 α -E2 on metabolic parameters in female WT and ER α KO mice provided a standard chow diet. In contrast to the males, we chose not to subject female WT and ER α KO mice to HFD because female ER α KO mice spontaneously develop obesity due to the ablation of ER α [52, 53]. Given that the female ER α KO mice are already in a challenged state, HFD would further exacerbate mass and adiposity differences between ER α KO and WT female mice. We found that 17 α -E2 failed to elicit improvements in mass, adiposity, calorie consumption, or metabolic parameters in female mice of either genotype (Figure 3-figure supplement 2). The positive effects of 17 α -E2 in male mice led us to speculate that the liver may play a key role in modulating 17 α -E2-mediated effects on systemic metabolic homeostasis. Importantly, several studies have implicated hepatic ER α in the regulation of glucose homeostasis, insulin sensitivity, and crosstalk with hypothalamic neurons that modulate metabolism and feeding behavior [42, 54, 55].

17 α -E2 improves liver disease pathology in an ER α -dependent manner in male mice

We previously reported that 17 α -E2 alters hepatic lipid deposition and DNA damage responses in male mice through unknown mechanisms [22]. In the current study we sought to determine if these findings are mediated through ER α . We found that 17 α -E2 significantly reduced liver mass and steatosis in male WT, but not ER α KO mice, as evidenced by reductions in oil-red-O positivity, fatty acid content, and triglyceride accumulation (Figure 4, Figure 4-figure supplement 1). These observations were accompanied by significant alterations in gene expression associated with *de novo* lipogenesis (fatty acid synthase [*Fasn*]) and β -oxidation (peroxisome proliferator-activated receptor alpha [*Ppara*]; sterol regulatory element binding transcription factor 1 [*Srebf1*]) (Figure 4-figure supplement 1). These findings are similar to previous reports showing that 17 β -E2 acts through ER α to modulate the expression and activity of genes that regulate hepatic lipid metabolism [56-58]. Interestingly, despite seeing overall reductions in hepatic fatty acid content with 17 α -E2 treatment in male WT mice (Figure 4C), we also observed elevations in specific fatty acids in these mice as compared to WT HFD controls. Notably, arachidonic acid (AA, 20:4n6) and docosahexaenoic acid (DHA, 22:6n3), both of which are precursors for eicosanoid, resolvin, and protectin production [59, 60], were found to be increased by 17 α -E2 treatment in male WT mice (Figure 4-figure supplement 2). Our findings are aligned with a previous report by

Garratt et al. showing that 17 α -E2 increases AA and DHA in liver [26]. None of the 17 α -E2-mediated changes in fatty acid profiles were observed in male ER α KO mice receiving 17 α -E2. In response to the elevations in AA and DHA with 17 α -E2 treatment, we also assessed circulating eicosanoids. We found that 17 α -E2 treatment also mildly altered several circulating eicosanoid concentrations in male WT mice (Supplementary File 2). Many of these have been linked to changes in inflammatory signaling [61, 62], although the role they are playing in 17 α -E2-mediated effects of on metabolism and/or aging remain unclear.

Due to the association between obesity-related hepatic steatosis and the onset of fibrosis, we assessed collagen deposition by trichrome staining and found that 17 α -E2 reduced this in male WT, but not ER α KO, mice (Figure 5A). We also observed significant suppression of several transcripts associated with liver fibrosis in male WT mice receiving 17 α -E2, including collagen type 1 alpha 1 (*Col1a1*) [63, 64], cyclin-dependent kinase inhibitor 1A (*Cdkn1a*) [65, 66], matrix metalloproteinase 1 (*Mmp1*) [67], matrix metalloproteinase 12 (*Mmp12*) [68], monocyte chemoattractant protein 1 (*Ccl2*) [69, 70], C-X-C motif chemokine ligand 1 (*Cxcl1*) [71], growth differentiation factor 15 (*Gdf15*) [72], and TNF receptor superfamily member 1A (*Tnfrsf1a*) [73] (Figure 5B). Transcripts shown to be predicative of hepatic insulin resistance (follistatin [*Fst*], inhibin subunit beta E [*Inhbe*], insulin receptor substrate 2 [*Irs2*]) [74, 75] and gluconeogenic plasticity (phosphoenolpyruvate carboxykinase 1 [*Pck1*], pyruvate kinase [*Pkm*]) [76] were also beneficially modulated by 17 α -E2 in male WT mice (Figure 4-figure supplement 1). To confirm that 17 α -E2 improves hepatic insulin sensitivity, we also evaluated phosphorylation status of AKT and FOXO1 in livers from male WT and ER α KO mice following the administration of an insulin bolus (Figure 5C). We found dramatic improvements in phosphorylated AKT (pS473) and FOXO1 (pS256) in male WT mice treated with 17 α -E2 (Figure 5D-E), whereas these benefits were not observed in male ER α KO mice. Our findings are aligned with previous reports demonstrating that hepatic ER α plays a critical role in regulating insulin sensitivity in the liver of male mice [39-41, 77]. Collectively, these findings suggest that the liver is highly responsive to 17 α -E2 and that hepatic ER α is likely the signaling mechanism by which 17 α -E2 prevents and/or reverses steatosis, fibrosis, and insulin resistance.

Despite our findings demonstrating that 17 α -E2 reduces calorie intake and improves liver disease parameters in male mice in an ER α dependent manner, it has historically been unclear if the benefits attributed to 17 α -E2 occur primarily due to long-term reductions in calorie intake. Moreover, it remains unclear if 17 α -E2 acts in a tissue-specific manner and if these observations would also occur in other mammalian species. To address these questions, we subsequently evaluated the effects of acute 17 α -E2 administration during hyperinsulinemic-euglycemic clamps in male WT outbred rats. These experiments allowed us to evaluate tissue-specific insulin-sensitivity following acute 17 α -E2 exposure, thereby circumventing long-term effects of the compound including reductions in calorie intake.

Acute 17 α -E2 administration improves hepatic insulin sensitivity in male rats

Our first set of experiments in male rats sought to determine if acute peripheral infusions of 17 α -E2 modulates metabolic parameters during hyperinsulinemic-euglycemic clamps (Figure 6A). We found that acute

peripheral administration of 17 α -E2 significantly increased systemic insulin responsiveness as compared to vehicle controls, which is indicated by increased glucose infusion rates (GIRs) (Figure 6B). These studies also determined that peripheral 17 α -E2 administration robustly suppressed hepatic gluconeogenesis (R_a ; Figure 6C-D), whereas glucose disposal rates (R_d ; Figure 6E) were essentially identical between groups under clamped conditions. These data indicate that 17 α -E2 beneficially modulates metabolic parameters independent of reductions in calorie intake and adiposity. Furthermore, these findings strongly suggest that the liver is a primary site where 17 α -E2 acts to improve metabolic homeostasis due to gluconeogenesis being tightly controlled by hormonal actions on hepatocytes [78]. However, it is also well-established that the hypothalamus can directly modulate gluconeogenesis in the liver through hepatic innervation [79], therefore we sought to determine if acute intracerebroventricular (ICV) delivery of 17 α -E2 (Figure 6F) could modulate metabolic parameters similarly to that observed during peripheral 17 α -E2 administration. Interestingly, we found that central administration of 17 α -E2 essentially phenocopied the effects of peripheral 17 α -E2 infusion with regard to GIRs and suppression of hepatic gluconeogenesis (Figure 6G-I). These findings suggest that 17 α -E2 likely acts through hypothalamic neurons to regulate hepatic gluconeogenesis. Indeed, agouti-related peptide/neuropeptide Y (AgRP/NPY) and pro-opiomelanocortin (Pomc) neurons are known to regulate hepatic glucose production [43-47] and both neuronal populations express ER α [80-86]. Collectively, the hyperinsulinemic-euglycemic clamp studies revealed that 17 α -E2 definitively modulates metabolic homeostasis in an acute manner, and suggests that the liver and hypothalamus are two primary sites of action for the regulation of metabolic parameters by 17 α -E2.

DISCUSSION

17 α -E2 has recently been found to increase median lifespan in male mice through uncharacterized mechanisms [20, 21]. We and others have shown that metabolic improvements by 17 α -E2 may underlie the lifespan extending effects. In these studies, we sought to determine the role of ER α in 17 α -E2-mediated transcriptional effects *in vitro* and metabolic effects *in vivo*. Although previous studies have shown that 17 α -E2 has limited binding affinity for ER α , it remains unclear if 17 α -E2 can induce transcriptional and physiological alterations in this manner. Given the close association between metabolic improvements and ER α activity, we hypothesized that 17 α -E2 signals through ER α to elicit beneficial health outcomes. In these studies, we utilized U2OS cells stably-expressing ER α and ER α global knockout mice to assess the involvement of this receptor in mediating 17 α -E2 effects. Results from these studies demonstrate that ER α plays a pivotal role in 17 α -E2-mediated effects on genomic activity and metabolism. Moreover, these data suggest that ER α may be a target for the treatment of aging and chronic diseases in males.

Given the similarities between the metabolic benefits observed *in vivo* with 17 α -E2 treatment and the established body of literature linking ER α activity to systemic metabolic regulation [55], we utilized a well-established cell line model to globally assess the ER α cistrome and transcriptome following 17 α -E2 and 17 β -E2 treatment. We found that, regardless of dose, 17 α -E2 and 17 β -E2 elicited the same pattern of ER α genomic

binding loci and these loci shared the same DNA motif enrichments. Additionally, activation and suppression of gene expression were similar with both 17α -E2 and 17β -E2 exposure and were independent of dosage. This provides strong evidence that 17α -E2 is likely signaling through ER α to elicit beneficial outcomes, which is contrary to what other reports have suggested [21, 25, 26, 29, 30, 87]. Toran-Allerand et al. reported that 17α -E2 signals through a novel receptor in the brain, which they termed ER-X [29, 87]. Although our findings appear to dispute this notion, several reports have shown that ER α exists and functions as multiple alternatively-spliced variants [88-92]. Therefore, we speculate that ER-X may have been a truncated, alternatively-spliced, form of ER α . These findings led us to investigate how ER α may modulate 17α -E2-induced benefits *in vivo* using ER α global KO mice.

In alignment with our previous reports [22, 23], 17α -E2 reduced calorie intake, body mass, adiposity, and obesity-related metabolic perturbations in male WT mice. Conversely, 17α -E2 failed to elicit these beneficial effects in ER α KO mice, further supporting our hypothesis that ER α is the receptor by which 17α -E2 signals to induce beneficial metabolic outcomes. These observations are similar to how ER α is known to mediate the actions of endogenous estrogens on metabolic parameters in females [55]. In particular, 17β -E2 acts through ER α to regulate systemic insulin sensitivity, lipid distribution, thermogenesis, and hypothalamic anorexigenic pathways [55, 93, 94]. The loss of endogenous estrogen action due to menopause in humans or ovariectomy (OVX) in rodents eliminates these beneficial effects and elicits metabolic perturbations [95]. Moreover, OVX following sexual maturation has also been shown to reduce lifespan in female mice [96], indicating that endogenous estrogens regulate lifespan in females; which we surmise is at least partially mediated through ER α . In the current study, 17α -E2 failed to induce beneficial metabolic effects in female mice of either genotype, which we postulate is due to 17β -E2 outcompeting 17α -E2 at classical estrogen receptors in female WT mice due to its higher binding affinity. As alluded to previously, reports in the literature indicate the binding affinity of 17β -E2 for ERs is dramatically greater than 17α -E2, which has been confirmed with competitive binding assays [32-35]. While our data shows similar genomic actions of ER α in response to 17α -E2 and 17β -E2 exposure, several recent reports provide evidence that genomic and non-genomic actions of ER α differentially regulate metabolism in a sex-specific manner [38, 97], which may be a potential explanation for why female mice remain predominantly unresponsive to 17α -E2 as compared to male mice. In males, very few studies have evaluated the role of ER α in metabolism, although a few recent reports have suggested that ER α plays tissue-specific roles, particularly in the liver, by regulating glucoregulatory pathways [38-42, 77]. These studies, coupled with our current findings, led us to speculate that 17α -E2 may be signaling through ER α in the liver to reverse metabolic disease and potentially extend healthspan and/or lifespan in males.

The liver is a major regulator of systemic metabolic homeostasis. Obesity and advancing age often promote a variety of liver conditions, including steatosis, fibrosis, and insulin resistance; all of which are associated with hallmarks of aging [98], including cellular senescence [99], epigenetic alterations [100], and

dysregulated nutrient-sensing [1]. We have previously shown that 17 α -E2 can reduce hepatic steatosis, hepatic insulin resistance, and hepatocyte DNA damage through unknown mechanisms [22]. In the present study, we sought to determine if these findings are mediated through ER α . We found that 17 α -E2 dramatically reduced liver mass and lipid content. As expected, these observations were not seen in ER α KO mice, providing further support for the hypothesis that 17 α -E2 regulates systemic metabolic parameters through ER α . Interestingly, our findings suggest that 17 α -E2 suppresses *de novo* lipogenesis and increases β -oxidation, predominantly in an ER α -dependent manner. This is aligned with previous reports showing that 17 β -E2 can modulate hepatic lipid dynamics through both genomic and non-genomic actions [97], leading to altered expression of rate limiting enzymes that control *de novo* lipogenesis [58] and β -oxidation [101]. Reports have also shown that 17 β -E2 can increase triglyceride export, thereby decreasing hepatic lipid deposition [102]. Although we did not directly assess cholesterol profiles in these studies, we speculate that 17 α -E2 may partially reduce hepatic steatosis by increasing VLDL synthesis and/or triglyceride incorporation into VLDL. Additional studies will be needed to confirm how 17 α -E2 alters hepatic lipoprotein dynamics.

Hepatic steatosis promotes liver fibrosis, which exacerbates hepatic insulin resistance [103]. Endogenous estrogens and hormone replacement therapies in post-menopausal women have been shown to serve a protective role on liver function [57, 101, 102, 104, 105]. Additionally, male humans are at a higher risk of developing hepatic steatosis and fibrosis as compared to age-matched females [106, 107]. In addition to reducing hepatic lipid deposition in male WT mice in the current studies, 17 α -E2 also dramatically suppressed transcriptional and histological markers of hepatic fibrosis in an ER α -dependent manner. We also determined that 17 α -E2 improved hepatic insulin sensitivity in male WT, but not ER α KO, mice. Several transcriptional markers associated with hepatic insulin resistance were suppressed in male WT mice receiving 17 α -E2, whereas this suppression was almost entirely absent in ER α KO mice. Subsequent studies employing insulin stimulation prior to euthanasia also revealed that 17 α -E2 robustly increased liver AKT and FOXO1 phosphorylation in male WT mice, indicating a reversal of obesity-related hepatic insulin resistance and increased control of gluconeogenesis. These findings clearly demonstrate that 17 α -E2 modulates hepatic insulin sensitivity in an ER α -dependent manner. These observations are aligned with previous reports showing that 17 β -E2 acts through ER α to improve glucoregulation [42, 102]. This provides further support that 17 α -E2 is eliciting metabolic improvements through ER α that are specific to the liver. Therefore, hepatic ER α may be a promising target for the development of therapeutics to alleviate metabolic disease in males. Future studies utilizing cell-type-specific ablation of ER α in the liver will be needed to unravel these possibilities.

Despite the robust effects of 17 α -E2 on liver function, it remained unclear if 17 α -E2 directly modulates hepatic insulin sensitivity or if these benefits were a secondary response to prolonged reductions in calorie intake, adiposity, and lipid redistribution. To test this, we performed hyperinsulinemic-euglycemic clamps, in conjunction with acute infusions of 17 α -E2 in male WT rats. We found that peripheral infusions of 17 α -E2 improved hepatic

insulin sensitivity almost immediately, as evidenced by a greater suppression of hepatic glucose production in rats receiving 17 α -E2 as compared to vehicle controls. Additionally, we did not observe improvements in glucose disposal, thereby indicating that 17 α -E2 does not acutely increase systemic insulin-stimulated glucose uptake. This observation is aligned with recent literature demonstrating limited involvement of ER α in skeletal muscle insulin sensitivity [108]. These data indicate that 17 α -E2 primarily alters systemic metabolic homeostasis through the modulation of hepatic gluconeogenesis, which is known to account for 76-87% of glucose production in the body [109]. Although these studies are suggestive of direct actions in the liver, 17 α -E2 also has the ability to cross the blood brain barrier and elicit responses in the hypothalamus [23]. Given that the hypothalamus can regulate hepatic glucose production [43-47, 79], we also evaluated systemic insulin sensitivity following central administration of 17 α -E2. These experiments essentially phenocopied the results of the peripheral 17 α -E2 infusions, suggesting that the suppression of hepatic gluconeogenesis by 17 α -E2 is at least partially mediated by the hypothalamus. A multitude of studies have shown that the arcuate nucleus (ARC) of the hypothalamus plays a critical role in the regulation of hepatic gluconeogenesis through autonomic regulation and vagus nerve activity [44, 45, 78, 110]. Multiple neuronal populations within the ARC are known to be involved in the regulation of hepatic glucose production, including Pomc [47] and AgRP/NPY [43-46]. Similarly, we have previously shown that the effects of 17 α -E2 on calorie intake and adiposity are dependent upon functional Pomc neurons, thereby providing evidence that 17 α -E2 can act through the hypothalamus to mediate systemic metabolic parameters [23]. However, in the absence of functional Pomc neurons, 17 α -E2 was still able to reduce fasting glucose and insulin, suggesting that 17 α -E2 modulates peripheral metabolism through multiple mechanisms, which may include alternative neuronal populations. Given that both Pomc [111] and AgRP/NPY [80, 81, 83-86, 112] neurons express ER α , regulate systemic metabolic parameters, and modulate feeding circuitry in a coordinated counter-regulatory fashion, it remains unclear whether 17 α -E2 is altering hepatic and systemic metabolic parameters through Pomc and/or AgRP/NPY neurons. Interestingly, a recent report from Debarba et al. demonstrated that 17 α -E2 increased hypothalamic ER α expression in the ARC [113], which further suggests that 17 α -E2 signals through ER α in the hypothalamus. Future studies utilizing hypothalamic cell-type-specific ER α KO models will be needed to disentangle which populations of neurons are required for 17 α -E2 to control food intake, peripheral glucose homeostasis, and insulin sensitivity.

Collectively, our findings strongly suggest that 17 α -E2 acts through ER α in the liver and/or hypothalamus to modulate metabolic parameters. However, our findings are in contrast to other reports suggesting that 17 α -E2 elicits health benefits by modulating androgen metabolism [25, 26]. Garratt et al. reported that responsiveness to 17 α -E2 was significantly attenuated in castrated male mice [26], which the authors proposed may indicate 17 α -E2 acts as a 5 α -reductase inhibitor [114] to prevent the conversion of testosterone into dihydrotestosterone (DHT). 17 α -E2 is known to be a mild 5 α -reductase inhibitor that is prescribed as a topical treatment for androgenetic alopecia [115]. 5 α -reductase inhibition could conceivably elicit beneficial metabolic effects by either reducing the concentration of DHT, which has been shown to decrease adiposity [116, 117], or by promoting

greater aromatization of testosterone to 17β -E2 [118], which has been linked to improvements in metabolic parameters [119]. If true, this would imply that the benefits of 17α -E2 are occurring in an indirect manner. However, the dose of 17α -E2 used in the vast majority of these studies, does not induce dramatic feminization of the sex hormone profiles in male mice [22], which leads us to speculate that 17α -E2 is acting in a direct manner through ER α rather than indirectly through androgen modulation. Furthermore, studies in male rodents [120, 121] and humans [122] demonstrate that 5α -reductase inhibition or deficiency increases insulin resistance and hepatic steatosis and fibrosis, which are contradictory to the effects of 17α -E2 treatment in all of our studies utilizing male mice [22-24, 123]. Despite these contrasting observations, the studies by Garratt et al. do provide important insights into the interconnected and underappreciated relationship between androgen- and estrogen-signaling pathways and their roles in metabolism and aging. For instance, several recent reports have demonstrated interactions between the androgen receptor (AR) and ER α [124-126], which suggests that modulation of one may affect function of the other. Additional factors to consider when comparing and contrasting our studies from those of Garratt et al. are differences in the length of study, age and obesity status of the mice, and counterregulatory and/or compensatory effects of castration. Notably, it is plausible that 17α -E2 could be inducing metabolic benefits and lifespan-extending effects through several distinct mechanisms, including direct actions through ER α , suppression of DHT production, and/or aromatization of testosterone. Future studies will be needed to discern the potentially interdependent nature of 17α -E2 actions on ER α and androgen metabolism in metabolic improvement and lifespan-extension.

There are a few notable caveats to our studies. First, we utilized constitutive global ER α KO mice, which have been shown to display varying degrees of compensatory ER β activity due to the absence of ER α during development [127, 128]. However, if compensatory ER β expression was playing a role in our study, we likely would not see a complete attenuation of 17α -E2 mediated effects. As such, the results of our studies clearly indicate that ER α is the primary receptor by which 17α -E2 signals. Another potential concern of the model is that ER α KO mice are known to have elevated endogenous testosterone levels [129], although the studies by Garratt et al. would suggest that higher testosterone levels could potentially render the male mice more responsive to 17α -E2, whereas we observed the opposite. Future studies utilizing inducible Cre models to knockdown ER α post-sexual development may be considered if it is determined that Cre induction and subsequent ER α ablation is consistent throughout multiple organ systems, which has been shown to be inconsistent in other reports [130]. Despite these minor concerns related to the model, the use of the constitutive global ER α KO was undoubtedly the best option for these studies. It must also be noted that female mice present a greater phenotypic response than males to the ablation of ER α , thereby exacerbating obesity and metabolic dysfunction which makes comparisons to female WT mice as well as their male littermates problematic [52, 53]. For this reason, we chose not to provide HFD to female mice in these studies. Regardless, 17α -E2 still failed to elicit beneficial responses in female mice of either genotype (WT or ER α KO) which is aligned with previous reports demonstrating a lack of effect of 17α -E2 in females [25, 26]; however, it remains unclear if 17α -E2 can beneficially affect female mice

under challenged conditions, such as HFD and/or OVX. Lastly, the current studies were relatively short in duration and it remains unclear if metabolic improvements with 17 α -E2 treatment are required for the lifespan extension effects of the compound. Although several other studies have evaluated the long-term effects of 17 α -E2 [20, 21, 25, 26], a shorter treatment duration was effective for testing our hypothesis in these studies. Similarly, given the close relationship between metabolic homeostasis, sex hormones, and longevity [1, 55], we surmise that future studies evaluating the effects of ER α on male lifespan in the presence or absence of 17 α -E2 will be needed. While our current report does not provide direct evidence that ER α modulates the lifespan extending effects of 17 α -E2, it does provide insight into the involvement of hepatic and/or hypothalamic ER α on 17 α -E2-mediated metabolic effects in male mice.

In summary, the data presented herein are the first to show that 17 α -E2 and 17 β -E2 induce nearly identical ER α chromatin association patterns and transcriptional activity. Moreover, we demonstrate that the metabolic benefits of 17 α -E2 in male mice are ER α -dependent. We also provide evidence that strongly suggests 17 α -E2 acts through the liver and hypothalamus to regulate metabolic homeostasis in male mice. These effects were mirrored by studies in male WT rats receiving 17 α -E2, indicating that 17 α -E2 can modulate metabolism almost instantaneously and that these effects are not limited to a single mammalian species. Future studies will be needed to confirm that 17 α -E2 acts predominantly through ER α in a cell-type-specific manner in the liver and hypothalamus to modulate systemic metabolic homeostasis. It is also imperative that we determine if ER α exclusively modulates the lifespan-extending effects of 17 α -E2 in male mice. Another potential avenue of investigation that remains unresolved is whether 17 α -E2 acts through ER α in a genomic or non-genomic manner to modulate health parameters. Potential interactions between androgen and estrogen signaling must also be considered when evaluating the effects of 17 α -E2 on metabolism and lifespan. These studies will provide additional insight into mechanisms of metabolic improvement and lifespan extension by 17 α -E2. Our studies provide critical insight into the molecular mechanisms by which 17 α -E2 elicits metabolic benefits in males, which were previously unknown and may underlie its lifespan extending effects.

METHODS

Key Resources Table				
Reagent type (species) or resource	Designation	Source or reference	Identifiers	Additional information
genetic reagent (<i>M. musculus</i>)	B6N(Cg)-Esr1 ^{tm4.2Ksk/J}	The Jackson Laboratory	Stock No:026176; RRID:IMSR_JAX:026176	ER α (<i>Esr1</i>) KO mice
cell line (<i>Homo sapien</i>)	U2OS Cells	ATCC	HTB-96; RRID:CVCL_0042	PMID: 15802376 PMID: 14505348
antibody	anti-FLAG M2 (Mouse monoclonal)	Sigma-Aldrich	F1804	IP: 1uL per pull-down (1mg/mL)
commercial assay or kit	Protein G Dynabeads	Applied Biosystems/ThermoFisher Scientific	10003D	IP: 30uL per IP
chemical compound, drug	17 α -E2	Steraloids, Inc	E0870-000	
chemical compound, drug	Novolin R 100 U/ml	Novolin		2mU/g
other (diet)	Chow; TestDiet 58YP	TestDiet	TestDiet 58YP	
other (diet)	HFD; TestDiet 58V8	TestDiet	TestDiet 58V8	HFD 45% by kcal
other (diet)	HFD; TestDiet 58Y1	TestDiet	TestDiet 58Y1	HFD 60% by kcal
commercial assay or kit	Mouse Ultrasensitive Insulin ELISA	ALPCO	Cat# 80-INSMSU-E01; RRID:AB_2792981	
commercial assay or kit	Free Glycerol Agent	Sigma-Aldrich	Sigma F6428	
commercial assay or kit	Triglyceride Reagent	Sigma-Aldrich	Sigma F6428	

commercial assay or kit	Glycerol Standard	Sigma-Aldrich	Sigma G1394	
antibody	anti-pS473 AKT (Rabbit polyclonal)	Abcam	Cat# ab81283; RRID:AB_2224551	WB: (1:3000)
antibody	anti-pan-AKT (Rabbit polyclonal)	Abcam	Cat# ab179463; RRID:AB_2810977	WB (1:10000)
antibody	anti-pS256 FOXO1 (Rabbit polyclonal)	Abcam	Cat# ab131339; RRID:AB_11159015	WB (1:1000)
antibody	anti-FOXO1a (Rabbit polyclonal)	Abcam	Cat# ab52857; RRID:AB_869817	WB (1:1000)
antibody	anti-GAPDH (Rabbit polyclonal)	Abcam	Cat# ab9485; RRID:AB_307275	WB (1:2500)
antibody	anti-Rabbit IgG, IRDye 800 CW	LI-COR	Cat# 926-32211; RRID:AB_621843	WB (1:15000)
commercial assay or kit	TaqMan Gene Expression Master Mix	Applied Biosystems/ Thermofisher Scientific	4369542	
sequenced-based reagent	qPCR primer <i>Mmp1</i>	Integrated DNA Technologies	Mm.PT.58.42286812 Ref Seq: NM_008607(1)	Exon 5-6
sequenced-based reagent	qPCR primer <i>Mmp12</i>	Integrated DNA Technologies	Mm.PT.58.31615472 Ref Seq: NM_008605(1)	Exon 8-9
sequenced-based reagent	qPCR primer <i>Ccl2</i>	Integrated DNA Technologies	Mm.PT.58.42151692 Ref Seq: NM_011333(1)	Exon 1-3
sequenced-based reagent	qPCR primer <i>Srebf1</i>	Integrated DNA Technologies	Mm.PT.58.8508227 Ref Seq: NM_011480(1)	Exon 1-2

sequenced-based reagent	qPCR primer <i>Pck1</i>	Integrated DNA Technologies	Mm.PT.58.11992693 Ref Seq: NM_011044(1)	Exon 3-4
sequenced-based reagent	qPCR primer <i>Cdkn1a</i>	Integrated DNA Technologies	Mm.PT.58.17125846 Ref Seq: NM_007669(1)	Exon 2-3
sequenced-based reagent	qPCR primer <i>Ppara</i>	Integrated DNA Technologies	Mm.PT.58.9374886 Ref Seq: NM_001113418(2)	Exon 8-9
sequenced-based reagent	qPCR primer <i>Cxcl1</i>	Integrated DNA Technologies	Mm.PT.58.42076891 Ref Seq: NM_008176(1)	Exon 2-4
sequenced-based reagent	qPCR primer <i>Col1a1</i>	Integrated DNA Technologies	Mm.PT.58.7562513 Ref Seq: M_007742(1)	Exon 1-2
sequenced-based reagent	qPCR primer <i>Tnfrsf1a</i>	Integrated DNA Technologies	Mm.PT.58.28810479 Ref Seq: NM_011609(1)	Exon 5-7
software, algorithm	SigmaPlot 12.5	Systat Software	RRID:SCR_003210	statistical analyses
software, algorithm	ImageJ	ImageJ	RRID:SCR_003070	histological quantification
software, algorithm	Image Studio	LI-COR	RRID:SCR_015795	western blot quantification
software, algorithm	RStudio	GenomicAlignments DiffBind DESeq2 GenomicRanges	RRID:SCR_000432	Peak Calling Differential expression Differential binding
software, algorithm	Bowtie2 MACS2	Bowtie2 MACS2		Alignment, Peak Calling,

	Bedtools Samtools Picard-tools Trimmomatic	Bedtools Samtools Picard-tools Trimmomatic		trimming, duplicate identification
--	-----------------------------------------------------	-----------------------------------------------------	--	------------------------------------------

U2OS Cells: U2OS osteosarcoma cells stably-expressing flag-tagged ER α (U2OS-ER α) under the control of doxycycline (dox) inducible promoter [48] were utilized for the studies described here. U2OS cells were originally purchased from ATTC and were authenticated using IDEXX BioAnalytics (Westbrook, ME). Cells were also regularly checked for mycoplasma contamination using a PCR based mycoplasma detection kit from SouthernBiotech (Birmingham, AL) and were confirmed to be negative. U2OS-ER α cells were cultured in phenol-free α MEM medium supplemented with 10% HyCloneTM charcoal/dextran stripped FBS (GE Healthcare Life Sciences, Pittsburgh, PA), 1% antibiotic/antimycotic, 5mg/L blasticidin S, and 500mg/L zeocin in a humidified 37°C incubator with 5% CO₂. Cells were plated in 12-well plates in the presence of doxycycline to induce ER α expression. The following day, cells were treated for 24 hours with 17 β -E2 (10nM) or 17 α -E2 (10nM and 100nM) (Steraloids, Newport, RI) in charcoal-stripped FBS-containing media.

ChIP-Sequencing: To evaluate patterns of ER α binding agonized by 17 α -E2 vs 17 β -E2, we performed ChIP-Sequencing. U2OS-ER α cells were harvested 24 hours post-treatment and chromatin immunoprecipitation was performed as previously described [131, 132]. Briefly, ER α was immunoprecipitated overnight at 4°C using 10 μ g of Flag antibody (clone M2, Sigma-Aldrich, St. Louis, MO). Complexes bound to the antibody were captured with protein G Dynabeads (Thermo Fisher Scientific, Waltham, MA), extensively washed, and reverse cross-linked at 65 °C overnight. DNA isolation was performed by phenol/chloroform extraction and was used for ChIP-sequencing library preparation. Libraries were sequenced using paired-end 100 bp reads on the Illumina HiSeq 4000 (GSE151039). Reads were aligned to the human genome (hg19, <https://genome.ucsc.edu/cgi-bin/hgGateway>) using bowtie2 [133] and duplicated reads were flagged with Picard-tools (<http://broadinstitute.github.io/picard/>). ER α binding peaks were called using MACS2 [134] with recommended settings. Peak genomic location, breadth of coverage, and peak summit location were determined using MACS2. NarrowPeak files containing peak information were used to determine differential ER α binding. Prior to differential binding analysis, peaks were centralized around the summit and 250bp flanking regions were added to the summit location to generate equal 500bp regions across treatment groups. Read counts were extracted for each peak from the aligned de-duplicated BAM file and were normalized to total library sequencing depth. To determine differential binding, the R package diffbind was utilized [135]. First, reads were log₂ transformed and normalized across all treatment groups. Differential binding between treatment groups was determined using generalized linear models utilized in the R package DESeq2. Significance threshold was set to false-discovery rate (FDR) corrected p-value < 0.05. Motif analysis was performed using HOMER with standard settings and all identified motifs are included in Supplementary File 1. Peak regions called for each treatment group were

analyzed to identify enriched motifs relative to the entire genome. Hypergeometric test was used to test enrichment. Only motifs with FDR corrected p-value < 0.05 were reported as significant.

RNA-Sequencing: U2OS-ER α cells were harvested 24 hours post-treatment and RNA was extracted using Trizol and DNase cleanup. RNA libraries were prepared with Illumina's TrueSeq RNA-seq library prep according to manufacturer protocol. Libraries were sequenced with 150bp paired-end reads on the Illumina 4000 platform (Illumina, San Diego, CA) (GSE151039). Sequence quality control was performed with fastQC, Paired reads were trimmed using trimmomatic, and were aligned to the hg19 genome using STAR [136]. Differential expression was determined using previously described methods [137]. In brief, gene counts were determined with the R package GenomicAlignments 'summarizeOverlap' function. Gene counts were then transformed using regularized log transformation and normalized relative to library size using the DESeq2 [138] R package. Differential expression was determined using negative binomial generalized linear model using *counts ~ treatment* model. All comparisons were corrected for multiple testing using Benjamini-Hochberg multiple testing correction method. Differential expression significance threshold was set to FDR corrected p-value < 0.05.

Animal Study 1: To determine if ER α is the primary receptor by which 17 α -E2 signals to elicit metabolic benefits *in vivo*, we utilized male global ER α KO and WT littermate mice. Mice were acquired from Dr. Kenneth Korach (National Institute of Environmental Health Sciences [NIEHS]) and were also bred at OUHSC by pairing ER α heterozygous KO mice (JAX; strain #026176). Mice were fed a 45% high-fat diet (HFD) (TestDiet 58V8, 35.5% CHO, 18.3% PRO, 45.7% FAT) \pm 17 α -E2 (14.4ppm; Steraloids, Newport, RI) from TestDiet (Richmond, IN) for 4 months prior to study initiation to induce obesity and metabolic perturbations. Additionally, age-matched, male WT, chow-fed mice were maintained on TestDiet 58YP (66.6% CHO, 20.4% PRO, 13.0% FAT) throughout the entire study as a healthy-weight reference group. Mice were individually housed with ISO cotton pad bedding, cardboard enrichment tubes, and nestlets at 22 \pm 0.5°C on a 12:12-hour light-dark cycle. Unless otherwise noted, all mice had ad libitum access to food and water throughout the experimental timeframe. At the conclusion of the fattening period, all mice (age: 6-8 months) receiving HFD were randomized within genotype by age, body mass, fat mass, calorie intake, fasting glucose, fasting insulin, and glycosylated hemoglobin (HbA1C) into HFD or HFD+17 α -E2 (TestDiet 58V8 + 17 α -E2, 14.4ppm; Steraloids, Newport, RI) treatment groups for a 14-week intervention. Body mass and calorie intake were assessed daily for the first 4 weeks, followed by body mass and body composition (EchoMRI, Houston, TX) on a weekly basis. At 10-weeks post-treatment, mice were fasted for 5-6 hours and fasting glucose, fasting insulin, and glucose tolerance were assessed. At the conclusion of the study (14-weeks post treatment), mice were euthanized with isoflurane in the fasted state (5-6 hours). Blood was collected into EDTA-lined tubes by cardiac puncture, and plasma was collected and frozen. Tissues were excised, weighed, flash frozen, and stored at -80°C unless otherwise noted. Small sections of liver were fixed in 4% paraformaldehyde in preparation for paraffin- or cryo-embedding for future analyses. All animal procedures were reviewed and approved by the Institutional Animal Care and Use Committee at OUHSC.

Animal Study 2: Although previous studies [20, 21, 25, 26] have demonstrated minimal effects of 17 α -E2 in female mice, we thought it prudent to determine if the ablation of ER α would alter female responsiveness to 17 α -E2. Female WT and ER α KO mice were acquired from Dr. Kenneth Korach (National Institute of Environmental Health Sciences [NIEHS]). Female mice were maintained on Chow TestDiet 58YP (66.6% CHO, 20.4% PRO, 13.0% FAT) and were not subject to HFD feeding due to ER α KO female mice naturally displaying an obesity phenotype. Mice were individually housed with ISO cotton pad bedding, cardboard enrichment tubes, and nestlets at 22 \pm 0.5°C on a 12:12-hour light-dark cycle. Unless otherwise noted, all mice had ad libitum access to food and water throughout the experimental timeframe. At age 9-11 months, female mice were randomized within genotype by age, body mass, fat mass, calorie intake, fasting glucose, fasting insulin, and glycosylated hemoglobin (HbA1C) into Chow or Chow+17 α -E2 (TestDiet 58YP + 17 α -E2, 14.4ppm; Steraloids, Newport, RI) treatment groups. The study was terminated following a 4-week intervention due to a lack of responsiveness to 17 α -E2. At the conclusion of the study, mice were euthanized with isoflurane in the fasted state (5-6 hours). Blood was collected into EDTA-lined tubes by cardiac puncture, and plasma was collected and frozen. Tissues were excised, weighed, flash frozen, and stored at -80°C. All animal procedures were reviewed and approved by the Institutional Animal Care and Use Committee at OUHSC.

Animal Study 3: To assess insulin sensitivity within the liver, an additional cohort of ER α KO and WT littermate mice were bred from mice acquired from Jackson Laboratory (JAX; strain #026176), which were generated from identical founder strains in the laboratory of Dr. Korach at NIEHS. Male ER α KO and WT mice were fed a 60% high-fat diet (HFD; TestDiet 58Y1, 20.3% CHO, 18.1% PRO, 61.6% FAT) for 4 months prior to study initiation to induce obesity and metabolic perturbations. Additionally, as was done in Animal Study 1, age-matched, male WT, chow-fed mice were maintained on TestDiet 58YP (66.6% CHO, 20.4% PRO, 13.0% FAT) throughout the entire study as a healthy-weight reference group. Mice were group housed with corncob bedding, cardboard enrichment tubes, and nestlets at 22 \pm 0.5°C on a 12:12-hour light-dark cycle. Unless otherwise noted, all mice had ad libitum access to food and water throughout the experimental timeframe. At the conclusion of the fattening period, all mice (age: 6 months) receiving HFD were randomized within genotype by body mass, fat mass, calorie intake, fasting glucose, and fasting insulin into HFD or HFD+17 α -E2 (TestDiet 58Y1 + 17 α -E2, 14.4ppm; Steraloids, Newport, RI) treatment groups for a 12-week intervention. Prior to being euthanized, mice were fasted (5-6 hours) and IP injected with insulin (Novolin R® 100 U/ml; 2mU/g) to assess insulin activity and sensitivity in tissue as previously described [139]. Each mouse was euthanized with isoflurane 15 minutes following their insulin injection. Blood was collected into EDTA-lined tubes by cardiac puncture, and plasma was collected and frozen. Tissues were excised, weighed, flash frozen, and stored at -80°C unless otherwise noted. All animal procedures were reviewed and approved by the Institutional Animal Care and Use Committee at OUHSC.

Animal Study 4: Hyperinsulinemic-euglycemic clamp experiments, the gold-standard for assessing insulin sensitivity, were performed in male rats to determine if 17 α -E2 can acutely modulate insulin sensitivity and glucose homeostasis. FBN-F1 hybrid male rats were acclimated to the animal facilities within the Einstein Nathan Shock Center for two weeks prior to undergoing surgeries in preparation for hyperinsulinemic-euglycemic clamp studies. Rats were fed Purina 5001 (58.0% CHO, 28.5% PRO, 13.5% FAT) and were individually housed with corncob bedding at 22 \pm 0.5°C on a 14:10-hour light-dark cycle with *ad libitum* access to food and water. All surgeries were conducted under 2% isoflurane. For clamp studies incorporating central infusions, rats underwent two surgical procedures. First, stereotactic placement of a steel-guide cannula (Plastics One, Roanoke, VA) reaching the 3rd ventricle was performed. The implant was secured in place with dental cement and animals were treated with analgesic as needed. Approximately 14 days later, animals underwent a second surgical procedure to place indwelling catheters into the right internal jugular vein and the left carotid artery, which was also performed for animals undergoing only peripheral clamp studies. Hyperinsulinemic-euglycemic clamp studies incorporating peripheral 17 α -E2 infusions were performed as previously described [140]. For studies employing peripheral infusions of 17 α -E2, 17 α -E2 was diluted in sterile saline to a final concentration of 30ng/ul. Beginning at t=0min animals received a primed-continuous infusion of saline or 30ng/ul 17 α -E2 provided as a 3ug bolus at a rate of 20ul/min over 5min, followed by a continuous infusion at a rate of 0.06ml/hr over 235min (9.4ng/hr) for a maintenance dose of 7ug (total dose 10ug). Hyperinsulinemic-euglycemic clamp studies with intracerebroventricular (ICV) infusions were performed as previously described [141]. 17 α -E2 powder (Steraloids, Newport, RI) was dissolved in DMSO at a concentration of 10mg/ml and stored at -80°C. For ICV infusions, 17 α -E2 was diluted in artificial cerebral spinal fluid (ACSF) to a final concentration of 2ng/ul. Beginning at t=0min, animals received a primed-continuous ICV infusion of ACSF (Veh.) or 17 α -E2 (17 α) provided as a 15ng bolus at a rate of 1ul/min over 7.5min, followed by a continuous infusion of 56.5ng at a rate of 0.08ul/hr over 6hr (9.4ng/hr) and a total dose of 71.5ng. All animal procedures were reviewed and approved by the Institutional Animal Care and Use Committee at the Einstein College of Medicine.

In Vivo Metabolic Analyses in Mice: To evaluate the effects of 17 α -E2 on metabolic parameters *in vivo*, we performed several assessments of glucose homeostasis. Unless otherwise noted, all experiments requiring fasting conditions were performed in the afternoon, 5-6 hours following the removal of food as outlined elsewhere [142]. To ensure fasting conditions, mice were transferred to clean cages containing ISO cotton padding and clean cardboard enrichment tubes. Non-terminal blood was collected via tail snip. Fasting glucose was evaluated using a Bayer Breeze 2 Blood Glucose Monitoring System (Bayer Global, Leverkusen, Germany). Fasting insulin was evaluated using a Mouse Ultrasensitive Insulin ELISA from Alpco (Salem, NH). HbA1c was assessed by A1C-Now Monitoring kits (Bayer, Whippany, NJ). Glucose tolerance tests were performed following a 5-hour fast using an intraperitoneal filtered dextrose injection of 1g/kg body mass [143]. Blood glucose was measured immediately pre-injection (time 0) and at 15, 30, 60, 90, and 120 minutes post injection.

Liver Histology: To evaluate the effects of 17 α -E2 treatment on lipid accumulation and fibrosis, we evaluated fixed liver tissue. Tissues were fixed in 4% PFA for 24 hours, cryo-embedding samples were transferred to 30% sucrose for 72 hours and embedded, paraffin-embedding samples were transferred to 1X PBS for 48 hours, then to 70% ethanol until embedding. Liver oil-red-O and Masson's trichrome staining were performed by the Oklahoma Medical Research Foundation Imaging Core Facility using previously reported methodology [144, 145]. Oil-red-O staining was performed on cryo-embedded tissue and was imaged within 6 hours of staining. Red lipid stain was blindly quantified from 10 images per animal using ImageJ software and presented as a lipid to total tissue ratio. Masson's trichrome staining was performed on paraffin embedded liver tissue and was used for qualitative purposes.

Liver Triglycerides: We evaluated the effects of 17 α -E2 treatment on triglyceride accumulation in the liver. Liver samples (~100 mg) were homogenized on ice for 60 seconds in 10X (v/w) Cell Signaling Lysis Buffer (Cell Signaling, Danvers, MA) with protease and phosphatase inhibitors (Boston BioProducts, Boston, MA). Total lipid was extracted from the homogenate using the Folch method with a 2:1 chloroform-methanol mixture [146]. Lipid was dried down using a nitrogen drier at room temperature, and resuspended in 100 μ L of 3:1:1 tert-butyl alcohol-methanol-Triton X-100 solution. Final triglyceride concentrations were determined using a spectrophotometric assay with a 4:1 Free Glycerol Agent / Triglyceride Agent solution (Sigma Triglyceride and Free-Glycerol reagents, St. Louis, MO) as previously described [147].

Liver Fatty Acids: We evaluated the effects of 17 α -E2 on hepatic fatty acid content. Liver samples (~50 mg) were homogenized and on ice for 60 seconds in 10X (v/w) Cell Signaling Lysis Buffer (Cell Signaling, Danvers, MA) with protease and phosphatase inhibitors (Boston BioProducts, Boston, MA). Total lipid was extracted using a modified Bligh and Dyer method [148] (Sigma-Aldrich, St. Louis, MO). 50nmol of 15:0 and 17:0 internal standards were added and acid hydrolysis/methanolysis was done to generate fatty acid methyl esters (FAMES) [149]. FAMES were identified as previously described by GC-MS [149]. A 6890N gas chromatograph with flame ionization detector (GC-FID) (Agilent Technologies) was used to quantify FAMES [150]. Standards 15:0 and 17:0 were used to compare and determine sample concentrations. Data is represented as the relative mole percent of each fatty acid.

Plasma Eicosanoids: We evaluated the effects of 17 α -E2 treatment on circulating eicosanoids (Supplementary File 2). Plasma eicosanoid analyses were performed by the UCSD Lipidomics Core as described previously [151]. Eicosanoids were isolated from plasma, extracted, separated using liquid chromatography, and analyzed with mass spectrometry (MDS SCIEX 4000 Q Trap; Applied Biosystems, Foster City, CA) [151].

Real-time PCR: To evaluate alterations in gene expression following 17 α -E2 treatment, we performed qPCR for genes related to fibrosis, lipid metabolism, insulin resistance, and glucose metabolism in the liver. Total RNA

was extracted using Trizol (Life Technologies, Carlsbad, CA) and was reverse transcribed to cDNA with the High-Capacity cDNA Reverse Transcription kit (Applied Biosystems, Foster City, CA). Real-time PCR was performed in a QuantStudio 12K Flex Real Time PCR System (ThermoFisher Scientific, Waltham, MA) using TaqMan™ Gene Expression Master Mix (Applied Biosystems/ThermoFisher Scientific, Waltham, MA) and predesigned gene expression assays with FAM probes from Integrated DNA Technologies (Skokie, Illinois). Target gene expression was expressed as $2^{-\Delta\Delta CT}$ by the comparative CT method [152] and normalized to the expression of TATA-Box Binding Protein (TBP) in liver.

Western Blotting: To determine if 17 α -E2 altered hepatic insulin sensitivity, we evaluated phosphorylation status of AKT and FOXO1 following an insulin bolus. Liver was homogenized in RIPA Buffer (Cell Signaling, Danvers, MA) with protease and phosphatase inhibitors (Boston Bioproducts, Boston, MA). Total protein was quantified using BCA Protein Assay Reagent Kit (Pierce, Rockford, IL). Proteins were separated on an Any kD™ Criterion™ TGX Stain-Free™ Protein Gel (Biorad, Hercules, CA) and transferred to nitrocellulose membranes, 0.2 μ m pore size (Biorad, Hercules, CA). Primary antibodies used were α -pS256 FOXO1 (Abcam ab131339, 1:1000), α -FOXO1a (Abcam ab52857, 1:1000), α -pS473 AKT (Abcam ab81283, 1:3000), α -pan-AKT (Abcam ab179463, 1:10000), α -GAPDH (Abcam ab9485, 1:2500). Primary antibody detection was performed with IRDye® 800CW Infrared α -Rabbit (LI-COR Biotechnology, Lincoln, NE) at 1:15000 concentration. Blot imaging was done on Odyssey Fc Imaging System (LI-COR Biotechnology, Lincoln, NE) and protein detection and quantification was performed with Image Studio Software (LI-COR Biotechnology, Lincoln, NE).

Statistical Analyses: Results are presented as mean \pm SEM unless otherwise stated with *p* values less than 0.05 considered to be significant unless otherwise specified. Analyses of differences between groups were performed by 2-way ANOVA, 2-way repeated measures ANOVA, or Student's t-test where appropriate using SigmaPlot 12.5 Software. A Benjamini-Hochberg multiple testing correction was applied to the F test result to correct for the number of transcripts, proteins, and fatty acids analyzed.

FIGURE LEGENDS

Figure 1. 17 α -E2 and 17 β -E2 elicit similar transcriptional profiles through ER α . (A) Heatmap representing normalized genome-wide DNA binding by ER α via ChIP sequencing analyses centered according to peak summits for each treatment group, (B) Motif enrichment analysis, filtered for mammalian and non-overlapping motif groups, showing the top 10 non-redundant enriched sequence motifs across treatment groups, (C) PCA plot of transcriptional profiles by RNA sequencing analyses, and (D) Heatmap representing differentially-expressed genes (FDR < 0.05) by RNA sequencing analyses (left) and ER α binding patterns within the gene body \pm 5 kb flanking regions of these genes identified by ChIP sequencing (right). These studies utilized U2OS-ER α cells treated with low dose (10nM) 17 α -E2, high dose (100nM) 17 α -E2, 17 β -E2 (10nM), or vehicle (EtOH). n=3/group.

Figure 1-figure supplement 1. 17 α -E2 and 17 β -E2 elicit similar ER α binding profile. PCA plot of genome-wide ER α binding profiles by ChIP sequencing analyses. U2OS-ER α cells treated with low dose (10nM) 17 α -E2, high dose (100nM) 17 α -E2, or 17 β -E2 (10nM) induced binding in common genomic locations and differed from vehicle (EtOH) treated cells. n=3/group.

Figure 2. ER α is required for 17 α -E2 to reduce mass, adiposity, and calorie intake in male mice. (A) Percent change in mass (mean \pm SEM, 2-way repeated measures ANOVA with Holm-Sidak post-hoc; * p<0.05, ** p<0.005 between WT HFD and WT 17 α), (B) Mass at baseline (week 0; solid) and week 14 (striped) (mean \pm SEM, 2-way repeated measures ANOVA with Holm-Sidak post-hoc; * p<0.05, ** p<0.005), (C) Percent change in fat mass (mean \pm SEM, 2-way repeated measures ANOVA with Holm-Sidak post-hoc; * p<0.05, ** p<0.005), (D) Fat mass at baseline (week 0; solid) and week 14 (striped) (mean \pm SEM, 2-way repeated measures ANOVA with Holm-Sidak post-hoc; * p<0.05, ** p<0.005), and (E) Average daily calorie intake per week in WT and ER α KO mice provided 45% HFD (TestDiet 58V8) \pm 17 α -E2 (14.4ppm) (mean \pm SEM, 2-way repeated measures ANOVA with Holm-Sidak post-hoc; * p<0.05, ** p<0.005). Age-matched, male WT, chow-fed (TestDiet 58YP) mice were also evaluated as a normal-weight reference group and the corresponding means are depicted as dashed grey lines. n = 10 (WT HFD), 10 (WT 17 α), 9 (KO HFD), 10 (KO 17 α), 12-15 (WT Chow).

Figure 3. 17 α -E2 reverses obesity-related metabolic dysfunction in male WT, but not ER α KO, mice. (A) Fasting glucose (mean \pm SEM, 2-way repeated measures ANOVA), (B) Fasting insulin (mean \pm SEM, 2-way repeated measures ANOVA with Holm-Sidak post-hoc; * p<0.05, ** p<0.005), and (C) glycosylated hemoglobin (HbA1c) at baseline (week 0; solid) and week 14 (striped) in WT and ER α KO mice provided 45% HFD (TestDiet 58V8) \pm 17 α -E2 (14.4 ppm) (mean \pm SEM, 2-way repeated measures ANOVA with Holm-Sidak post-hoc; ** p<0.005). (D) Glucose tolerance testing (GTT; 1mg/kg) (mean \pm SEM, 2-way repeated measures ANOVA with Holm-Sidak post-hoc; * p<0.05 between WT HFD and WT 17 α), and (E) GTT AUC during week 10 of the study (mean \pm SEM, 2-way ANOVA with Holm-Sidak post-hoc; * p<0.05). Age-matched, male WT, chow-fed (TestDiet 58YP) mice were also evaluated as a normal-weight reference group and the corresponding means are depicted as dashed grey lines. n = 9-10 (WT HFD), 8-10 (WT 17 α), 9-10 (KO HFD), 8-10 (KO 17 α), 12-15 (WT Chow).

Figure 3-figure supplement 1. 17 α -E2 reverses obesity-related metabolic dysfunction in male WT, but not ER α KO, mice. (A) Glucose tolerance testing (GTT; 1mg/kg), normalized to baseline (min 0) (mean \pm SEM,

2-way repeated measures ANOVA with Holm-Sidak post-hoc; * $p < 0.05$ between WT HFD and WT 17 α , and (B) Normalized GTT AUC in WT and ER α KO mice provided 45% HFD (TestDiet 58V8) \pm 17 α -E2 (14.4ppm) for 10 weeks (mean \pm SEM, 2-way ANOVA with Holm-Sidak post-hoc; * $p < 0.05$). Age-matched, male WT, chow-fed (TestDiet 58YP) mice were also evaluated as a normal-weight reference group and the corresponding means are depicted as dashed grey lines. $n = 10$ (WT HFD), 8 (WT 17 α), 9 (KO HFD), 8 (KO 17 α), 12 (WT Chow).

Figure 3-figure supplement 2. 17 α -E2 fails to alter metabolic parameters in WT or ER α KO female mice.

(A) Mass at baseline (week 0; solid) and week 4 (striped) (mean \pm SEM, 2-way repeated measures ANOVA), (B) Fat mass at baseline (week 0; solid) and week 4 (striped) (mean \pm SEM, 2-way repeated measures ANOVA), (C) Average daily calorie intake per week (mean \pm SEM, 2-way repeated measures ANOVA), (D) Fasting glucose during week 4 (mean \pm SEM, 2-way repeated measures ANOVA), and (E) Fasting insulin during week 4 in WT and ER α KO female mice provided chow (TestDiet 58YP) \pm 17 α -E2 (14.4ppm) (mean \pm SEM, 2-way repeated measures ANOVA). $n = 9$ (WT Chow), 9 (WT 17 α), 11 (KO Chow), 9 (KO 17 α).

Figure 4. 17 α -E2 reverses obesity-related hepatic steatosis in an ER α -dependent manner in male mice.

(A) Liver mass (mean \pm SEM, 2-way ANOVA with Holm-Sidak post-hoc; * $p < 0.05$), (B) Representative liver oil-red-O staining, (C) Liver fatty acids (mean \pm SEM, 2-way ANOVA with Holm-Sidak post-hoc; ** $p < 0.005$), and (D) Liver triglycerides in WT and ER α KO mice provided 45% HFD (TestDiet 58V8) \pm 17 α -E2 (14.4ppm) for 14 weeks (mean \pm SEM, 2-way ANOVA with Holm-Sidak post-hoc; ** $p < 0.005$). Age-matched, male WT, chow-fed (TestDiet 58YP) mice were also evaluated as a normal-weight reference group and the corresponding means are depicted as dashed grey lines. $n = 4-10$ (WT HFD), 4-9 (WT 17 α), 4-9 (KO HFD), 4-10 (KO 17 α), 4-15 (WT Chow).

Figure 4-figure supplement 1. 17 α -E2 alters markers of lipid and glucose homeostasis predominantly through in male mice.

(A) Quantification of oil-red-O lipid staining in liver sections from WT and ER α KO mice provided 45% HFD (TestDiet 58V8) \pm 17 α -E2 (14.4ppm) for 14 weeks (mean \pm SEM, 2-way ANOVA with Holm-Sidak post-hoc; * $p < 0.05$). Hepatic gene expression related to (B) Lipid metabolism (box plots depict total range of fold changes in gene expression with mean shown as a horizontal black line, Benjamini–Hochberg multiple testing correction, 2-way ANOVA with Holm-Sidak post-hoc; * $p < 0.05$, ** $p < 0.005$), (C) Hepatic insulin resistance (box plots depict total range of fold changes in gene expression with mean shown as a horizontal black line, Benjamini–Hochberg multiple testing correction, 2-way ANOVA with Holm-Sidak post-hoc; * $p < 0.05$, ** $p < 0.005$), and (D) Glucose homeostasis from WT and ER α KO mice provided 45% HFD (TestDiet 58V8) \pm 17 α -E2 (14.4ppm) for 14 weeks (box plots depict total range of fold changes in gene expression with mean shown as a horizontal black line, Benjamini–Hochberg multiple testing correction, 2-way ANOVA with Holm-Sidak post-hoc; * $p < 0.05$, ** $p < 0.005$). Age-matched, male WT, chow-fed (TestDiet 58YP) mice were also evaluated as a normal-weight reference group and the corresponding means are depicted as dashed grey lines. $n = 5-10$ (WT HFD), 5-9 (WT 17 α), 5-7 (KO HFD), 5-10 (KO 17 α), 8-11 (WT Chow).

Figure 4-figure supplement 2. 17 α -E2 alters the hepatic fatty acid profile in male WT, but not ER α KO, mice. Relative molar % of fatty acids in the liver from WT and ER α KO mice provided 45% HFD (TestDiet 58V8) \pm 17 α -E2 (14.4ppm) for 14 weeks (mean \pm SEM, Benjamini–Hochberg multiple testing correction, 2-way ANOVA

with Holm-Sidak post-hoc; * $p < 0.05$, ** $p < 0.005$). Age-matched, male WT, chow-fed (TestDiet 58YP) mice were also evaluated as a normal-weight reference group and the corresponding means are depicted as dashed grey lines. $n = 4$.

Figure 5. 17 α -E2 reverses obesity-related liver fibrosis and insulin resistance in an ER α -dependent manner in male mice. (A) Representative liver Masson's trichrome staining for collagen and (B) Liver transcriptional markers of fibrosis in WT and ER α KO mice provided 45% HFD (TestDiet 58V8) \pm 17 α -E2 (14.4ppm) for 14 weeks (box plots depict total range of fold changes in gene expression with mean shown as a horizontal black line, Benjamini–Hochberg multiple testing correction, 2-way ANOVA with Holm-Sidak post-hoc; * $p < 0.05$, ** $p < 0.005$). (C) Schematic of *in vivo* insulin stimulation (2mU/g) in fasting mice, (D) Representative liver immunoblots, and (E) Quantification of phospho/total (p/t) AKT (pS473) and FOXO1 (pS256) in WT and ER α KO mice provided 60% HFD (TestDiet 58Y1) \pm 17 α -E2 (14.4ppm) for 12 weeks (mean \pm SEM, Benjamini–Hochberg multiple testing correction, 2-way ANOVA with Holm-Sidak post-hoc; ** $p < 0.005$). Age-matched, male WT, chow-fed (TestDiet 58YP) mice were also evaluated as a normal-weight reference group and the corresponding means are depicted as dashed grey lines. $n = 7-10$ (WT HFD), 8-9 (WT 17 α), 7-10 (KO HFD), 10 (KO 17 α), 7-11 (WT Chow).

Figure 6. Acute delivery of 17 α -E2 improves hepatic insulin sensitivity. (A) Schematic of peripheral 17 α -E2 infusions (or vehicle) during hyperinsulinemic-euglycemic clamps, (B) Glucose infusion rates (GIR) (mean \pm SEM, unpaired Student's t-test; ** $p < 0.005$), (C) Rate of glucose appearance (R_a ; hepatic glucose production) (mean \pm SEM, unpaired Student's t-test on Clamp; ** $p < 0.005$), (D) % suppression of hepatic glucose production (mean \pm SEM, unpaired Student's t-test; ** $p < 0.005$), and (E) Rate of glucose disappearance (R_d ; peripheral glucose disposal) in 6-month old, male, FBN-F1 hybrid rats (mean \pm SEM, unpaired Student's t-test on Clamp). (F) Schematic of ICV (central) 17 α -E2 infusions (or vehicle) during hyperinsulinemic-euglycemic clamps, (G) GIR (mean \pm SEM, unpaired Student's t-test; * $p < 0.05$), (H) R_a (mean \pm SEM, unpaired Student's t-test on Clamp; ** $p < 0.005$), (I) % suppression glucose production (mean \pm SEM, unpaired Student's t-test; * $p < 0.05$), and (J) R_d in 6-month old, male, FBN-F1 hybrid rats (mean \pm SEM, unpaired Student's t-test on Clamp). $n = 5-9$ (CON), 7-8 (17 α).

Supplementary File 1. Motif enrichment results. Complete and un-curated list of significant transcription factor motifs enriched within ER α binding sites following 17 α -E2, 17 β -E2 or vehicle (EtOH) treatment.

Supplementary File 2. Circulating eicosanoid levels (pmol/ml). 17 α -E2 mildly alters the circulating eicosanoid profile in obese middle-aged male mice. WT mice were provided 45% HFD (TestDiet 58V8) \pm 17 α -E2 (14.4ppm) for 14 weeks. Age-matched, male WT, chow-fed (TestDiet 58YP) mice were also evaluated as a normal-weight reference group. All data are presented as mean \pm SEM and were analyzed by Student's t-test with the WT Chow group being excluded from statistical comparisons. $n = 5-7$.

ACKNOWLEDGEMENTS

We thank Dr. Kenneth Korach at the National Institute of Environmental Health Sciences for providing ER α KO and WT littermate mice. We also thank Dr. Lora Bailey-Downs, Richard Brush, and Michael Sullivan for technical support. This work was supported by the National Institutes of Health (R00 AG51661 and R01 AG069742 to M.B.S., T32 AG052363 to S.N.M., R01 EY030513 to M-P.A., & R01 AG059430 to W.M.F.), Veterans Affairs (I01BX003906 to W.M.F) and pilot research funding from the Harold Hamm Diabetes Center (M.B.S. and S.N.M.), Einstein Nathan Shock Center (P30 AG038072) of Excellence in the Basic Biology of Aging (M.B.S.), and OUHSC Lipidomics Core (P30 EY012190).

COMPETING INTERESTS

The authors declare no conflicts or competing interests.

REFERENCES

1. Lopez-Otin, C., et al., *The hallmarks of aging*. Cell, 2013. **153**(6): p. 1194-217.
2. Villareal, D.T., et al., *Obesity in older adults: technical review and position statement of the American Society for Nutrition and NAASO, The Obesity Society*. Obesity research, 2005. **13**(11): p. 1849-63.
3. Waters, D.L., A.L. Ward, and D.T. Villareal, *Weight loss in obese adults 65years and older: a review of the controversy*. Exp Gerontol, 2013. **48**(10): p. 1054-61.
4. Flegal, K.M., et al., *Prevalence and trends in obesity among US adults, 1999-2008*. JAMA, 2010. **303**(3): p. 235-41.
5. Flegal, K.M., et al., *Trends in Obesity Among Adults in the United States, 2005 to 2014*. JAMA, 2016. **315**(21): p. 2284-91.
6. Bischof, G.N. and D.C. Park, *Obesity and Aging: Consequences for Cognition, Brain Structure, and Brain Function*. Psychosom Med, 2015. **77**(6): p. 697-709.
7. Horvath, S., et al., *Obesity accelerates epigenetic aging of human liver*. Proceedings of the National Academy of Sciences of the United States of America, 2014. **111**(43): p. 15538-43.
8. Nevalainen, T., et al., *Obesity accelerates epigenetic aging in middle-aged but not in elderly individuals*. Clin Epigenetics, 2017. **9**: p. 20.
9. Yang, H., et al., *Obesity accelerates thymic aging*. Blood, 2009. **114**(18): p. 3803-12.
10. Whitmer, R.A., et al., *Obesity in middle age and future risk of dementia: a 27 year longitudinal population based study*. BMJ, 2005. **330**(7504): p. 1360.
11. Whitmer, R.A., et al., *Midlife cardiovascular risk factors and risk of dementia in late life*. Neurology, 2005. **64**(2): p. 277-81.
12. Dye, L., et al., *The relationship between obesity and cognitive health and decline*. Proc Nutr Soc, 2017. **76**(4): p. 443-454.
13. Salvestrini, V., C. Sell, and A. Lorenzini, *Obesity May Accelerate the Aging Process*. Front Endocrinol (Lausanne), 2019. **10**: p. 266.
14. Tzanetakou, I.P., et al., *"Is obesity linked to aging?": adipose tissue and the role of telomeres*. Ageing research reviews, 2012. **11**(2): p. 220-9.
15. Perez, L.M., et al., *'Adipaging': ageing and obesity share biological hallmarks related to a dysfunctional adipose tissue*. J Physiol, 2016. **594**(12): p. 3187-207.
16. Tchkonja, T., et al., *Fat tissue, aging, and cellular senescence*. Aging cell, 2010. **9**(5): p. 667-84.
17. Stout, M.B., et al., *Physiological Aging: Links Among Adipose Tissue Dysfunction, Diabetes, and Frailty*. Physiology (Bethesda), 2017. **32**(1): p. 9-19.
18. Jensen, M.D., et al., *2013 AHA/ACC/TOS guideline for the management of overweight and obesity in adults: a report of the American College of Cardiology/American Heart Association Task Force on Practice Guidelines and The Obesity Society*. Circulation, 2014. **129**(25 Suppl 2): p. S102-38.
19. Dirks, A.J. and C. Leeuwenburgh, *Caloric restriction in humans: potential pitfalls and health concerns*. Mechanisms of ageing and development, 2006. **127**(1): p. 1-7.
20. Strong, R., et al., *Longer lifespan in male mice treated with a weakly estrogenic agonist, an antioxidant, an alpha-glucosidase inhibitor or a Nrf2-inducer*. Aging Cell, 2016. **15**(5): p. 872-84.
21. Harrison, D.E., et al., *Acarbose, 17-alpha-estradiol, and nordihydroguaiaretic acid extend mouse lifespan preferentially in males*. Aging cell, 2014. **13**(2): p. 273-82.
22. Stout, M.B., et al., *17alpha-Estradiol Alleviates Age-related Metabolic and Inflammatory Dysfunction in Male Mice Without Inducing Feminization*. J Gerontol A Biol Sci Med Sci, 2017. **72**(1): p. 3-15.
23. Steyn, F.J., et al., *17alpha-estradiol acts through hypothalamic pro-opiomelanocortin expressing neurons to reduce feeding behavior*. Aging Cell, 2018. **17**(1).
24. Miller, B.F., et al., *Short-term calorie restriction and 17alpha-estradiol administration elicit divergent effects on proteostatic processes and protein content in metabolically active tissues*. J Gerontol A Biol Sci Med Sci, 2019.
25. Garratt, M., et al., *Sex differences in lifespan extension with acarbose and 17-alpha estradiol: gonadal hormones underlie male-specific improvements in glucose tolerance and mTORC2 signaling*. Aging Cell, 2017. **16**(6): p. 1256-1266.
26. Garratt, M., et al., *Male lifespan extension with 17-alpha estradiol is linked to a sex-specific metabolomic response modulated by gonadal hormones in mice*. Aging Cell, 2018. **17**(4): p. e12786.

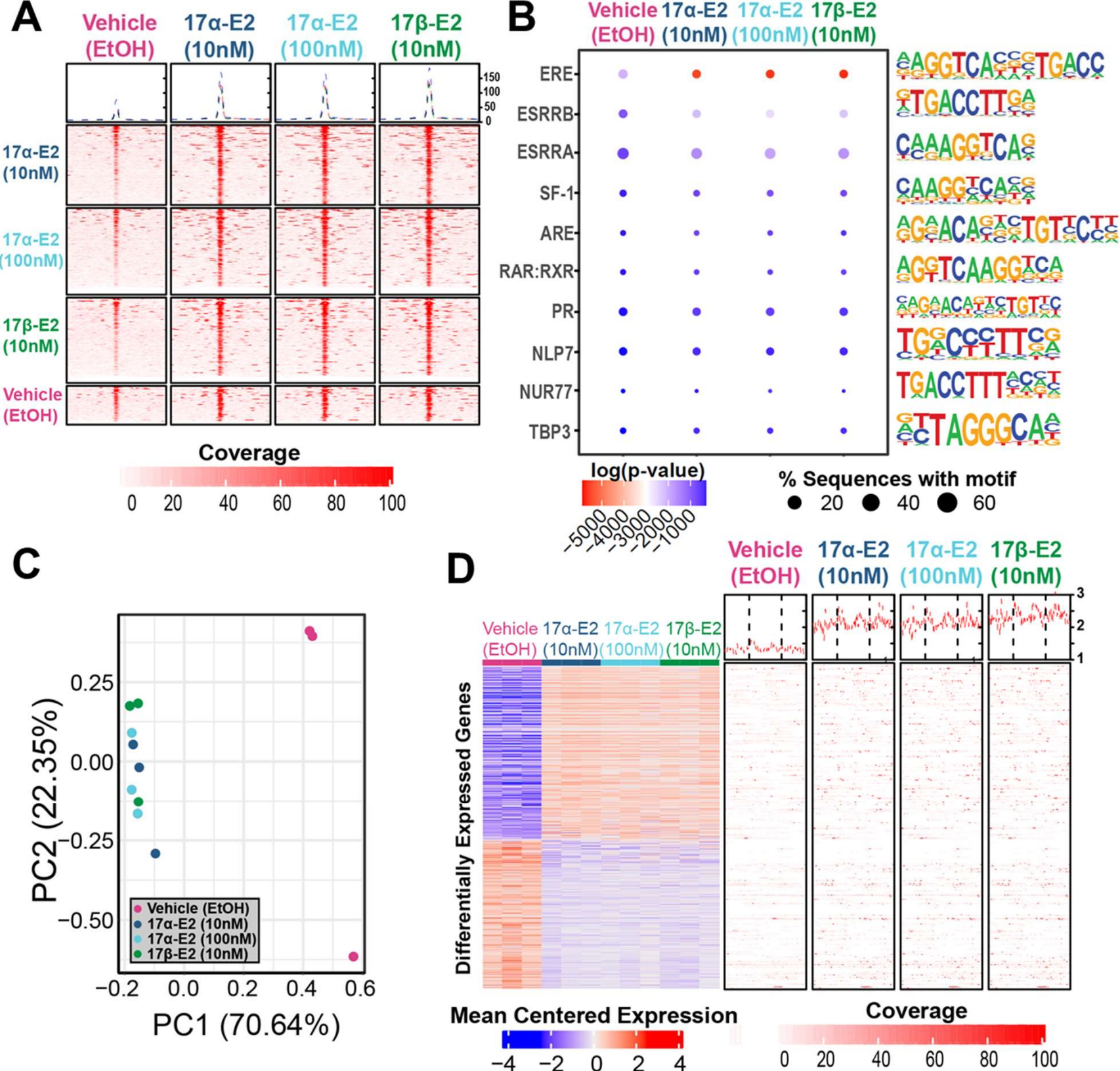
27. Tyshkovskiy, A., et al., *Identification and Application of Gene Expression Signatures Associated with Lifespan Extension*. Cell Metab, 2019. **30**(3): p. 573-593 e8.
28. Toran-Allerand, C.D., *Estrogen and the brain: beyond ER-alpha, ER-beta, and 17beta-estradiol*. Annals of the New York Academy of Sciences, 2005. **1052**: p. 136-44.
29. Toran-Allerand, C.D., et al., *ER-X: a novel, plasma membrane-associated, putative estrogen receptor that is regulated during development and after ischemic brain injury*. J Neurosci, 2002. **22**(19): p. 8391-401.
30. Toran-Allerand, C.D., et al., *17alpha-estradiol: a brain-active estrogen?* Endocrinology, 2005. **146**(9): p. 3843-50.
31. Green, P.S. and J.W. Simpkins, *Estrogens and estrogen-like non-feminizing compounds. Their role in the prevention and treatment of Alzheimer's disease*. Annals of the New York Academy of Sciences, 2000. **924**: p. 93-8.
32. Edwards, D.P. and W.L. McGuire, *17 alpha-Estradiol is a biologically active estrogen in human breast cancer cells in tissue culture*. Endocrinology, 1980. **107**(4): p. 884-91.
33. Korenman, S.G., *Comparative binding affinity of estrogens and its relation to estrogenic potency*. Steroids, 1969. **13**(2): p. 163-77.
34. Littlefield, B.A., et al., *A simple and sensitive microtiter plate estrogen bioassay based on stimulation of alkaline phosphatase in Ishikawa cells: estrogenic action of delta 5 adrenal steroids*. Endocrinology, 1990. **127**(6): p. 2757-62.
35. Anstead, G.M., K.E. Carlson, and J.A. Katzenellenbogen, *The estradiol pharmacophore: ligand structure-estrogen receptor binding affinity relationships and a model for the receptor binding site*. Steroids, 1997. **62**(3): p. 268-303.
36. Engler-Chiurazzi, E.B., D.F. Covey, and J.W. Simpkins, *A novel mechanism of non-feminizing estrogens in neuroprotection*. Exp Gerontol, 2016.
37. Kaur, S.P., S. Bansal, and K. Chopra, *17alpha-Estradiol: a candidate neuroserm and non-feminizing estrogen for postmenopausal neuronal complications*. Steroids, 2015. **96**: p. 7-15.
38. Allard, C., et al., *Loss of Nuclear and Membrane Estrogen Receptor-alpha Differentially Impairs Insulin Secretion and Action in Male and Female Mice*. Diabetes, 2019. **68**(3): p. 490-501.
39. Yan, H., et al., *Estrogen Improves Insulin Sensitivity and Suppresses Gluconeogenesis via the Transcription Factor Foxo1*. Diabetes, 2019. **68**(2): p. 291-304.
40. Guillaume, M., et al., *Selective Liver Estrogen Receptor alpha Modulation Prevents Steatosis, Diabetes, and Obesity Through the Anorectic Growth Differentiation Factor 15 Hepatokine in Mice*. Hepatol Commun, 2019. **3**(7): p. 908-924.
41. Qiu, S., et al., *Hepatic estrogen receptor alpha is critical for regulation of gluconeogenesis and lipid metabolism in males*. Sci Rep, 2017. **7**(1): p. 1661.
42. Meda, C., et al., *Hepatic ERalpha accounts for sex differences in the ability to cope with an excess of dietary lipids*. Mol Metab, 2020. **32**: p. 97-108.
43. Konner, A.C., et al., *Insulin action in AgRP-expressing neurons is required for suppression of hepatic glucose production*. Cell Metab, 2007. **5**(6): p. 438-49.
44. Ruud, J., S.M. Stecutorum, and J.C. Bruning, *Neuronal control of peripheral insulin sensitivity and glucose metabolism*. Nat Commun, 2017. **8**: p. 15259.
45. Pocai, A., et al., *A brain-liver circuit regulates glucose homeostasis*. Cell Metab, 2005. **1**(1): p. 53-61.
46. Pocai, A., et al., *Hypothalamic K(ATP) channels control hepatic glucose production*. Nature, 2005. **434**(7036): p. 1026-31.
47. Dodd, G.T., et al., *Insulin regulates POMC neuronal plasticity to control glucose metabolism*. Elife, 2018. **7**.
48. Monroe, D.G., et al., *Estrogen receptor isoform-specific regulation of endogenous gene expression in human osteoblastic cell lines expressing either ERalpha or ERbeta*. J Cell Biochem, 2003. **90**(2): p. 315-26.
49. Monroe, D.G., et al., *Estrogen receptor alpha and beta heterodimers exert unique effects on estrogen- and tamoxifen-dependent gene expression in human U2OS osteosarcoma cells*. Mol Endocrinol, 2005. **19**(6): p. 1555-68.
50. Lin, C.Y., et al., *Whole-genome cartography of estrogen receptor alpha binding sites*. PLoS Genet, 2007. **3**(6): p. e87.

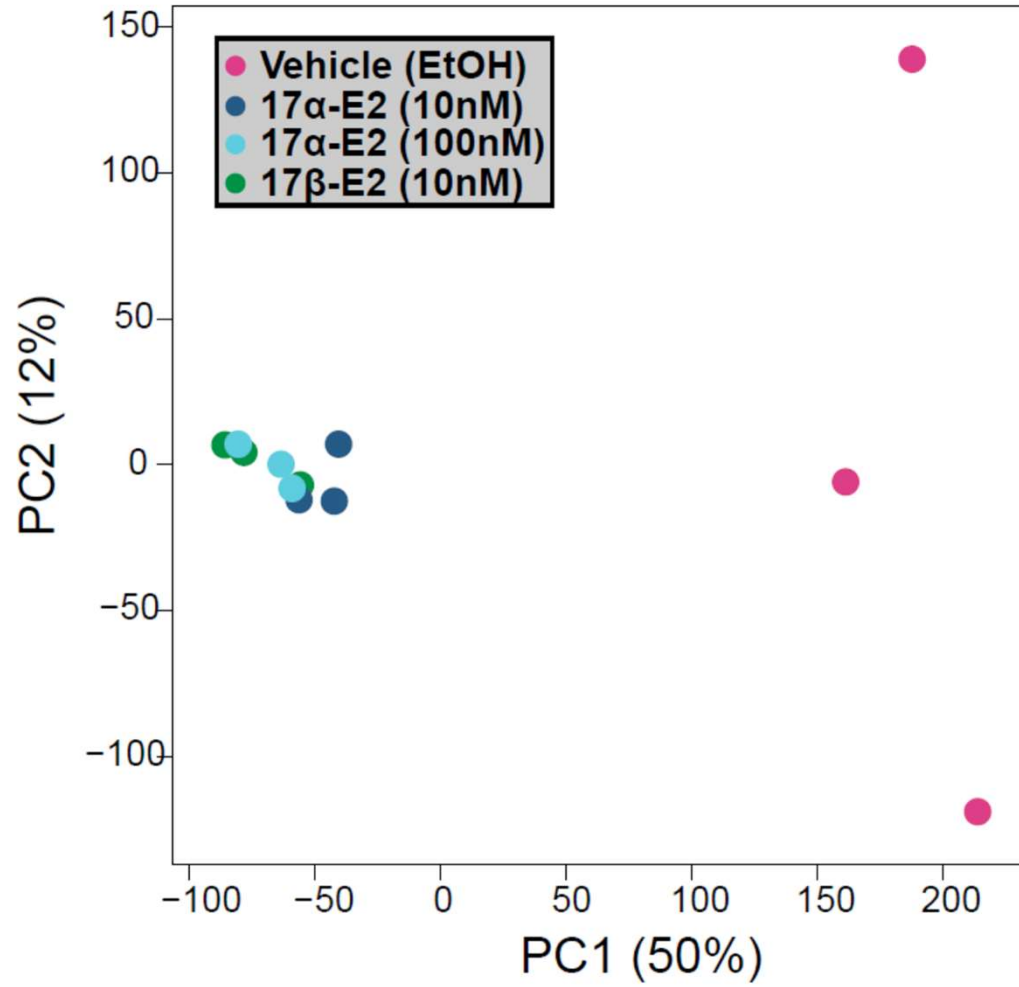
51. Lee, S.K., et al., *Estrogen receptor, a common interaction partner for a subset of nuclear receptors*. Mol Endocrinol, 1998. **12**(8): p. 1184-92.
52. Manrique, C., et al., *Loss of Estrogen Receptor alpha Signaling Leads to Insulin Resistance and Obesity in Young and Adult Female Mice*. Cardiorenal Med, 2012. **2**(3): p. 200-210.
53. Vidal, O., et al., *Disproportional body growth in female estrogen receptor-alpha-inactivated mice*. Biochem Biophys Res Commun, 1999. **265**(2): p. 569-71.
54. Torre, D., et al., *Sexual Dimorphism and Estrogen Action in Mouse Liver*. Adv Exp Med Biol, 2017. **1043**: p. 141-151.
55. Barros, R.P. and J.A. Gustafsson, *Estrogen receptors and the metabolic network*. Cell Metab, 2011. **14**(3): p. 289-99.
56. Della Torre, S., et al., *An Essential Role for Liver ERalpha in Coupling Hepatic Metabolism to the Reproductive Cycle*. Cell Rep, 2016. **15**(2): p. 360-71.
57. Stubbins, R.E., et al., *Estrogen modulates abdominal adiposity and protects female mice from obesity and impaired glucose tolerance*. Eur J Nutr, 2012. **51**(7): p. 861-70.
58. Zhang, H., et al., *Differential effects of estrogen/androgen on the prevention of nonalcoholic fatty liver disease in the male rat*. J Lipid Res, 2013. **54**(2): p. 345-57.
59. Szeffel, J., W.J. Kruszewski, and E. Sobczak, *Factors influencing the eicosanoids synthesis in vivo*. Biomed Res Int, 2015. **2015**: p. 690692.
60. Kohli, P. and B.D. Levy, *Resolvins and protectins: mediating solutions to inflammation*. Br J Pharmacol, 2009. **158**(4): p. 960-71.
61. Kiss, L., et al., *Epoxyeicosatrienoates are the dominant eicosanoids in human lungs upon microbial challenge*. Eur Respir J, 2010. **36**(5): p. 1088-98.
62. Gilroy, D.W., et al., *CYP450-derived oxylipins mediate inflammatory resolution*. Proc Natl Acad Sci U S A, 2016. **113**(23): p. E3240-9.
63. Hayashi, M., et al., *Identification of the collagen type 1 alpha 1 gene (COL1A1) as a candidate survival-related factor associated with hepatocellular carcinoma*. BMC Cancer, 2014. **14**: p. 108.
64. Lua, I., et al., *Characterization of hepatic stellate cells, portal fibroblasts, and mesothelial cells in normal and fibrotic livers*. J Hepatol, 2016. **64**(5): p. 1137-1146.
65. Crary, G.S. and J.H. Albrecht, *Expression of cyclin-dependent kinase inhibitor p21 in human liver*. Hepatology, 1998. **28**(3): p. 738-43.
66. Yang, L., et al., *Tbeta4 suppresses lincRNA-p21-mediated hepatic apoptosis and fibrosis by inhibiting PI3K-AKT-NF-kappaB pathway*. Gene, 2020. **758**: p. 144946.
67. Lichtinghagen, R., et al., *Expression and coordinated regulation of matrix metalloproteinases in chronic hepatitis C and hepatitis C virus-induced liver cirrhosis*. Clin Sci (Lond), 2003. **105**(3): p. 373-82.
68. Madala, S.K., et al., *Matrix metalloproteinase 12-deficiency augments extracellular matrix degrading metalloproteinases and attenuates IL-13-dependent fibrosis*. J Immunol, 2010. **184**(7): p. 3955-63.
69. Glass, O., et al., *Serum Interleukin-8, Osteopontin, and Monocyte Chemoattractant Protein 1 Are Associated With Hepatic Fibrosis in Patients With Nonalcoholic Fatty Liver Disease*. Hepatol Commun, 2018. **2**(11): p. 1344-1355.
70. Baeck, C., et al., *Pharmacological inhibition of the chemokine CCL2 (MCP-1) diminishes liver macrophage infiltration and steatohepatitis in chronic hepatic injury*. Gut, 2012. **61**(3): p. 416-26.
71. Yang, L., et al., *TRIF Differentially Regulates Hepatic Steatosis and Inflammation/Fibrosis in Mice*. Cell Mol Gastroenterol Hepatol, 2017. **3**(3): p. 469-483.
72. Koo, B.K., et al., *Growth differentiation factor 15 predicts advanced fibrosis in biopsy-proven non-alcoholic fatty liver disease*. Liver Int, 2018. **38**(4): p. 695-705.
73. Grattagliano, I., et al., *Targeting mitochondria to oppose the progression of nonalcoholic fatty liver disease*. Biochem Pharmacol, 2019. **160**: p. 34-45.
74. Tao, R., et al., *Inactivating hepatic follistatin alleviates hyperglycemia*. Nat Med, 2018. **24**(7): p. 1058-1069.
75. Parks, B.W., et al., *Genetic architecture of insulin resistance in the mouse*. Cell Metab, 2015. **21**(2): p. 334-347.
76. Xiong, Y., et al., *Regulation of glycolysis and gluconeogenesis by acetylation of PKM and PEPCK*. Cold Spring Harb Symp Quant Biol, 2011. **76**: p. 285-9.

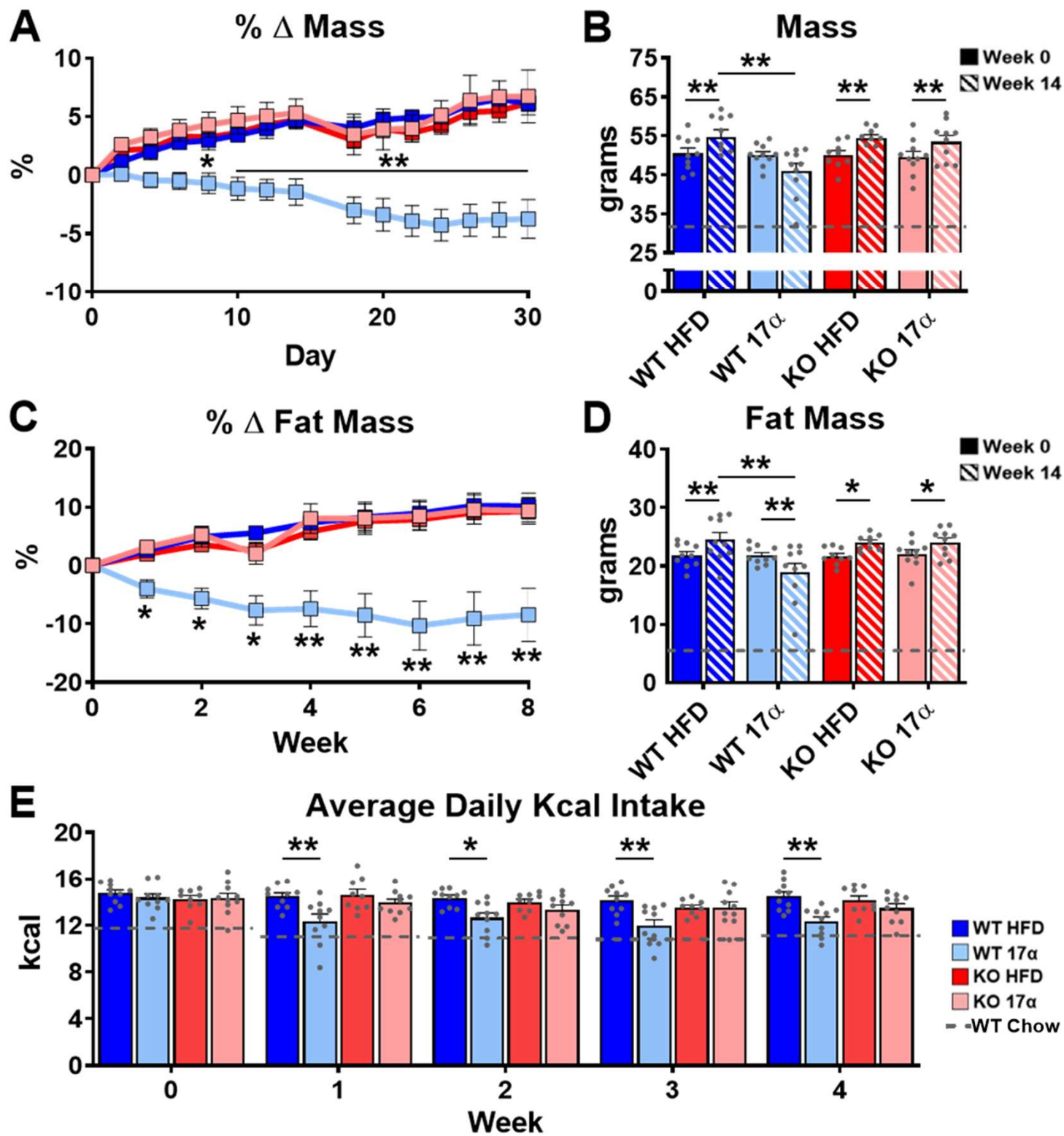
77. Zhu, L., et al., *Estrogen signaling prevents diet-induced hepatic insulin resistance in male mice with obesity*. Am J Physiol Endocrinol Metab, 2014. **306**(10): p. E1188-97.
78. Zhang, X., et al., *Unraveling the Regulation of Hepatic Gluconeogenesis*. Front Endocrinol (Lausanne), 2018. **9**: p. 802.
79. Timper, K. and J.C. Bruning, *Hypothalamic circuits regulating appetite and energy homeostasis: pathways to obesity*. Dis Model Mech, 2017. **10**(6): p. 679-689.
80. Smith, A.W., et al., *The membrane estrogen receptor ligand STX rapidly enhances GABAergic signaling in NPY/AgRP neurons: role in mediating the anorexigenic effects of 17beta-estradiol*. Am J Physiol Endocrinol Metab, 2013. **305**(5): p. E632-40.
81. Skinner, D.C. and A.E. Herbison, *Effects of photoperiod on estrogen receptor, tyrosine hydroxylase, neuropeptide Y, and beta-endorphin immunoreactivity in the ewe hypothalamus*. Endocrinology, 1997. **138**(6): p. 2585-95.
82. Xu, Y., et al., *Distinct hypothalamic neurons mediate estrogenic effects on energy homeostasis and reproduction*. Cell metabolism, 2011. **14**(4): p. 453-65.
83. Acosta-Martinez, M., T. Horton, and J.E. Levine, *Estrogen receptors in neuropeptide Y neurons: at the crossroads of feeding and reproduction*. Trends Endocrinol Metab, 2007. **18**(2): p. 48-50.
84. Stincic, T.L., O.K. Ronnekleiv, and M.J. Kelly, *Diverse actions of estradiol on anorexigenic and orexigenic hypothalamic arcuate neurons*. Horm Behav, 2018.
85. Kelly, M.J. and O.K. Ronnekleiv, *Minireview: neural signaling of estradiol in the hypothalamus*. Mol Endocrinol, 2015. **29**(5): p. 645-57.
86. Smith, A.W., O.K. Ronnekleiv, and M.J. Kelly, *Gq-mER signaling has opposite effects on hypothalamic orexigenic and anorexigenic neurons*. Steroids, 2014. **81**: p. 31-5.
87. Toran-Allerand, C.D., *Estrogen and the brain: beyond ER-alpha, ER-beta, and 17beta-estradiol*. Ann N Y Acad Sci, 2005. **1052**: p. 136-44.
88. Flouriot, G., et al., *Differentially expressed messenger RNA isoforms of the human estrogen receptor-alpha gene are generated by alternative splicing and promoter usage*. Mol Endocrinol, 1998. **12**(12): p. 1939-54.
89. Wang, Z., et al., *Identification, cloning, and expression of human estrogen receptor-alpha36, a novel variant of human estrogen receptor-alpha66*. Biochem Biophys Res Commun, 2005. **336**(4): p. 1023-7.
90. Taylor, S.E., P.L. Martin-Hirsch, and F.L. Martin, *Oestrogen receptor splice variants in the pathogenesis of disease*. Cancer Lett, 2010. **288**(2): p. 133-48.
91. Zhang, J., et al., *Alternative splicing of estrogen receptor alpha in hepatocellular carcinoma*. BMC Cancer, 2016. **16**(1): p. 926.
92. Lin, A.H., et al., *Differential ligand binding affinities of human estrogen receptor-alpha isoforms*. PLoS One, 2013. **8**(4): p. e63199.
93. Stincic, T.L., O.K. Ronnekleiv, and M.J. Kelly, *Diverse actions of estradiol on anorexigenic and orexigenic hypothalamic arcuate neurons*. Horm Behav, 2018. **104**: p. 146-155.
94. Lopez, M. and M. Tena-Sempere, *Estrogens and the control of energy homeostasis: a brain perspective*. Trends Endocrinol Metab, 2015. **26**(8): p. 411-21.
95. Stefanska, A., K. Bergmann, and G. Sypniewska, *Metabolic Syndrome and Menopause: Pathophysiology, Clinical and Diagnostic Significance*. Adv Clin Chem, 2015. **72**: p. 1-75.
96. Benedusi, V., et al., *Ovariectomy shortens the life span of female mice*. Oncotarget, 2015. **6**(13): p. 10801-11.
97. Pedram, A., et al., *Membrane and nuclear estrogen receptor alpha collaborate to suppress adipogenesis but not triglyceride content*. FASEB J, 2016. **30**(1): p. 230-40.
98. Hunt, N.J., et al., *Hallmarks of Aging in the Liver*. Comput Struct Biotechnol J, 2019. **17**: p. 1151-1161.
99. Ogrodnik, M., et al., *Cellular senescence drives age-dependent hepatic steatosis*. Nat Commun, 2017. **8**: p. 15691.
100. Horvath, S., et al., *Obesity accelerates epigenetic aging of human liver*. Proc Natl Acad Sci U S A, 2014. **111**(43): p. 15538-43.
101. Camporez, J.P., et al., *Cellular mechanism by which estradiol protects female ovariectomized mice from high-fat diet-induced hepatic and muscle insulin resistance*. Endocrinology, 2013. **154**(3): p. 1021-8.

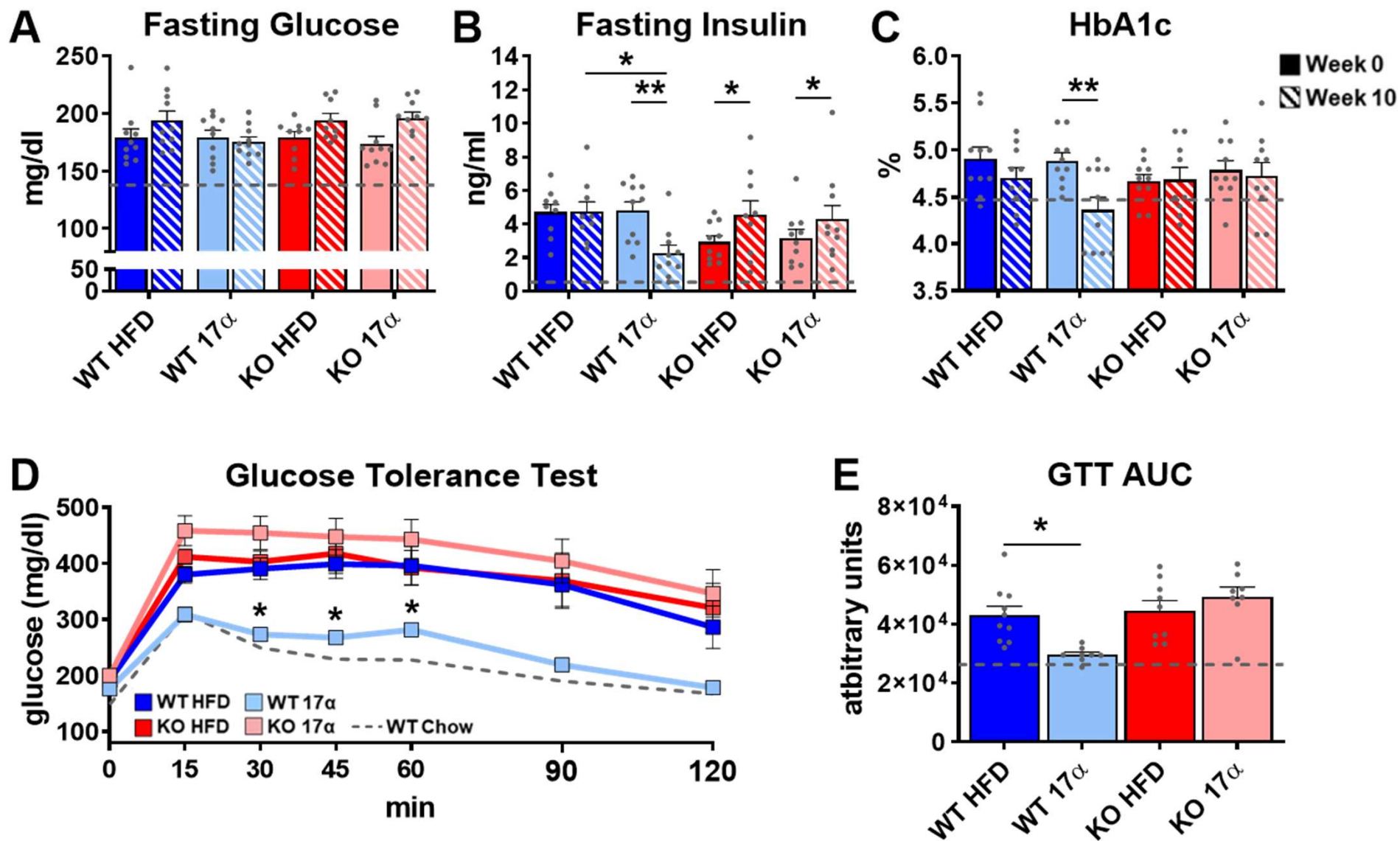
102. Zhu, L., et al., *Estrogen treatment after ovariectomy protects against fatty liver and may improve pathway-selective insulin resistance*. *Diabetes*, 2013. **62**(2): p. 424-34.
103. Kim, I.H., T. Kisseleva, and D.A. Brenner, *Aging and liver disease*. *Curr Opin Gastroenterol*, 2015. **31**(3): p. 184-91.
104. Rossi, R., G. Origliani, and M.G. Modena, *Transdermal 17-beta-estradiol and risk of developing type 2 diabetes in a population of healthy, nonobese postmenopausal women*. *Diabetes Care*, 2004. **27**(3): p. 645-9.
105. Brussaard, H.E., et al., *Short-term oestrogen replacement therapy improves insulin resistance, lipids and fibrinolysis in postmenopausal women with NIDDM*. *Diabetologia*, 1997. **40**(7): p. 843-9.
106. Guy, J. and M.G. Peters, *Liver disease in women: the influence of gender on epidemiology, natural history, and patient outcomes*. *Gastroenterol Hepatol (N Y)*, 2013. **9**(10): p. 633-9.
107. Collaborators, G.B.D.C., *The global, regional, and national burden of cirrhosis by cause in 195 countries and territories, 1990-2017: a systematic analysis for the Global Burden of Disease Study 2017*. *Lancet Gastroenterol Hepatol*, 2020. **5**(3): p. 245-266.
108. Inigo, M.R., et al., *Estrogen receptor-alpha in female skeletal muscle is not required for regulation of muscle insulin sensitivity and mitochondrial regulation*. *Mol Metab*, 2020. **34**: p. 1-15.
109. Cherrington, A.D., D.H. Wasserman, and O.P. McGinness, *Renal contribution to glucose production after a brief fast: fact or fancy?* *J Clin Invest*, 1994. **93**(6): p. 2303.
110. Brandt, C., et al., *Food Perception Primes Hepatic ER Homeostasis via Melanocortin-Dependent Control of mTOR Activation*. *Cell*, 2018. **175**(5): p. 1321-1335 e20.
111. Xu, Y., et al., *Distinct hypothalamic neurons mediate estrogenic effects on energy homeostasis and reproduction*. *Cell Metab*, 2011. **14**(4): p. 453-65.
112. Sar, M., et al., *Localization of neuropeptide-Y immunoreactivity in estradiol-concentrating cells in the hypothalamus*. *Endocrinology*, 1990. **127**(6): p. 2752-6.
113. Debarba, L.K., et al., *Sex hormones underlying 17 α -Estradiol effects on neuroinflammation*. *bioRxiv*, 2020: p. 2020.05.26.117689.
114. Schriefers, H., et al., *[Inhibition of testosterone metabolism by 17-alpha-estradiol in rat liver slices]*. *Arzneimittelforschung*, 1991. **41**(11): p. 1186-9.
115. Orfanos, C.E. and L. Vogels, *[Local therapy of androgenetic alopecia with 17 alpha-estradiol. A controlled, randomized double-blind study (author's transl)]*. *Dermatologica*, 1980. **161**(2): p. 124-32.
116. Moverare-Skrtic, S., et al., *Dihydrotestosterone treatment results in obesity and altered lipid metabolism in orchidectomized mice*. *Obesity (Silver Spring)*, 2006. **14**(4): p. 662-72.
117. Bolduc, C., et al., *Effects of dihydrotestosterone on adipose tissue measured by serial analysis of gene expression*. *J Mol Endocrinol*, 2004. **33**(2): p. 429-44.
118. Veldhuis, J.D., et al., *Aromatase and 5alpha-reductase inhibition during an exogenous testosterone clamp unveils selective sex steroid modulation of somatostatin and growth hormone secretagogue actions in healthy older men*. *J Clin Endocrinol Metab*, 2009. **94**(3): p. 973-81.
119. Rubinow, K.B., *Estrogens and Body Weight Regulation in Men*. *Adv Exp Med Biol*, 2017. **1043**: p. 285-313.
120. Livingstone, D.E., et al., *5alpha-Reductase type 1 deficiency or inhibition predisposes to insulin resistance, hepatic steatosis, and liver fibrosis in rodents*. *Diabetes*, 2015. **64**(2): p. 447-58.
121. Dowman, J.K., et al., *Loss of 5alpha-reductase type 1 accelerates the development of hepatic steatosis but protects against hepatocellular carcinoma in male mice*. *Endocrinology*, 2013. **154**(12): p. 4536-47.
122. Wei, L., et al., *Incidence of type 2 diabetes mellitus in men receiving steroid 5alpha-reductase inhibitors: population based cohort study*. *BMJ*, 2019. **365**: p. 11204.
123. Sidhom, S., et al., *17alpha-estradiol modulates IGF1 and hepatic gene expression in a sex-specific manner*. *J Gerontol A Biol Sci Med Sci*, 2020.
124. D'Amato, N.C., et al., *Cooperative Dynamics of AR and ER Activity in Breast Cancer*. *Mol Cancer Res*, 2016. **14**(11): p. 1054-1067.
125. Panet-Raymond, V., et al., *Interactions between androgen and estrogen receptors and the effects on their transactivational properties*. *Mol Cell Endocrinol*, 2000. **167**(1-2): p. 139-50.
126. Peters, A.A., et al., *Androgen receptor inhibits estrogen receptor-alpha activity and is prognostic in breast cancer*. *Cancer Res*, 2009. **69**(15): p. 6131-40.

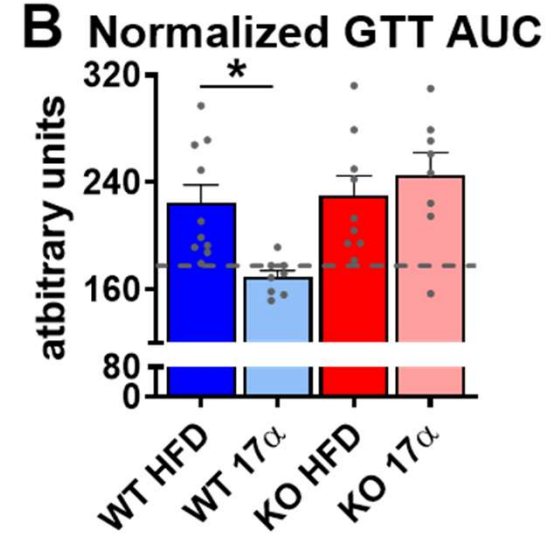
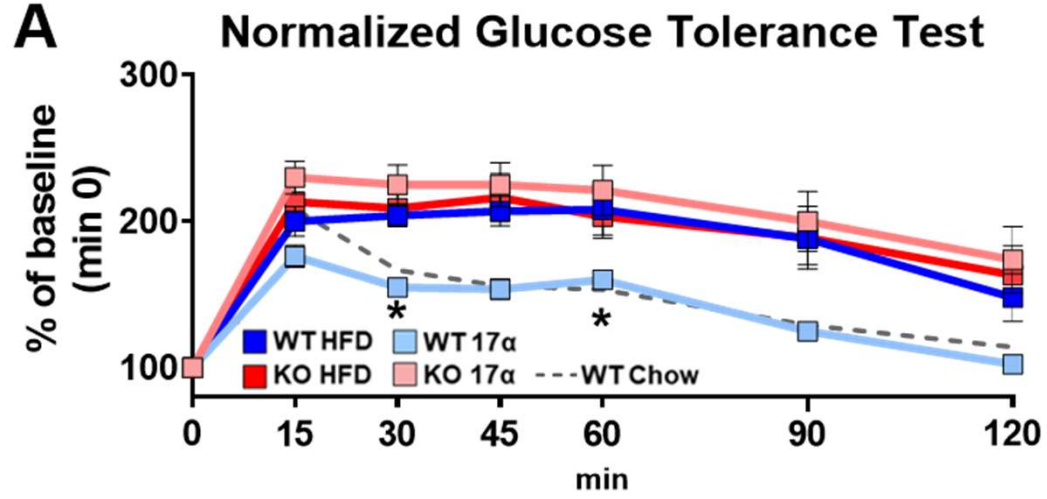
127. Sanchez-Criado, J.E., et al., *Estrogen receptor (ESR) 2 partially offsets the absence of ESR1 in gonadotropes of pituitary-specific Esr1 knockout female mice*. *Reproduction*, 2012. **143**(4): p. 549-58.
128. Rosenfeld, C.S., et al., *Transcription and translation of estrogen receptor-beta in the male reproductive tract of estrogen receptor-alpha knock-out and wild-type mice*. *Endocrinology*, 1998. **139**(6): p. 2982-7.
129. Gould, M.L., P.R. Hurst, and H.D. Nicholson, *The effects of oestrogen receptors alpha and beta on testicular cell number and steroidogenesis in mice*. *Reproduction*, 2007. **134**(2): p. 271-9.
130. Murray, S.A., et al., *Beyond knockouts: cre resources for conditional mutagenesis*. *Mamm Genome*, 2012. **23**(9-10): p. 587-99.
131. Reese, J.M., et al., *ERbeta-mediated induction of cystatins results in suppression of TGFbeta signaling and inhibition of triple-negative breast cancer metastasis*. *Proc Natl Acad Sci U S A*, 2018. **115**(41): p. E9580-E9589.
132. Nelson, J.D., et al., *Fast chromatin immunoprecipitation assay*. *Nucleic Acids Res*, 2006. **34**(1): p. e2.
133. Langmead, B. and S.L. Salzberg, *Fast gapped-read alignment with Bowtie 2*. *Nat Methods*, 2012. **9**(4): p. 357-9.
134. Zhang, Y., et al., *Model-based analysis of ChIP-Seq (MACS)*. *Genome Biol*, 2008. **9**(9): p. R137.
135. Ross-Innes, C.S., et al., *Differential oestrogen receptor binding is associated with clinical outcome in breast cancer*. *Nature*, 2012. **481**(7381): p. 389-93.
136. Dobin, A., et al., *STAR: ultrafast universal RNA-seq aligner*. *Bioinformatics*, 2013. **29**(1): p. 15-21.
137. Hadad, N., et al., *Early-life DNA methylation profiles are indicative of age-related transcriptome changes*. *Epigenetics Chromatin*, 2019. **12**(1): p. 58.
138. Love, M.I., W. Huber, and S. Anders, *Moderated estimation of fold change and dispersion for RNA-seq data with DESeq2*. *Genome Biol*, 2014. **15**(12): p. 550.
139. Lu, M., et al., *Insulin regulates liver metabolism in vivo in the absence of hepatic Akt and Foxo1*. *Nat Med*, 2012. **18**(3): p. 388-95.
140. Einstein, F.H., et al., *Aging per se increases the susceptibility to free fatty acid-induced insulin resistance*. *J Gerontol A Biol Sci Med Sci*, 2010. **65**(8): p. 800-8.
141. Huffman, D.M., et al., *Central insulin-like growth factor-1 (IGF-1) restores whole-body insulin action in a model of age-related insulin resistance and IGF-1 decline*. *Aging Cell*, 2016. **15**(1): p. 181-6.
142. Ayala, J.E., et al., *Standard operating procedures for describing and performing metabolic tests of glucose homeostasis in mice*. *Dis Model Mech*, 2010. **3**(9-10): p. 525-34.
143. Huffman, D.M., et al., *Evaluating Health Span in Preclinical Models of Aging and Disease: Guidelines, Challenges, and Opportunities for Geroscience*. *J Gerontol A Biol Sci Med Sci*, 2016. **71**(11): p. 1395-1406.
144. Leonard, A.K., et al., *Methods for the visualization and analysis of extracellular matrix protein structure and degradation*. *Methods Cell Biol*, 2018. **143**: p. 79-95.
145. Mehlem, A., et al., *Imaging of neutral lipids by oil red O for analyzing the metabolic status in health and disease*. *Nat Protoc*, 2013. **8**(6): p. 1149-54.
146. Folch, J., M. Lees, and G.H. Sloane Stanley, *A simple method for the isolation and purification of total lipides from animal tissues*. *The Journal of biological chemistry*, 1957. **226**(1): p. 497-509.
147. Stout, M.B., L.F. Liu, and M.A. Belury, *Hepatic steatosis by dietary-conjugated linoleic acid is accompanied by accumulation of diacylglycerol and increased membrane-associated protein kinase C epsilon in mice*. *Mol Nutr Food Res*, 2011. **55**(7): p. 1010-7.
148. Bligh, E.G. and W.J. Dyer, *A rapid method of total lipid extraction and purification*. *Can J Biochem Physiol*, 1959. **37**(8): p. 911-7.
149. Agbaga, M.P., et al., *Differential composition of DHA and very-long-chain PUFAs in rod and cone photoreceptors*. *J Lipid Res*, 2018. **59**(9): p. 1586-1596.
150. Yu, M., et al., *ELOVL4 protein preferentially elongates 20:5n3 to very long chain PUFAs over 20:4n6 and 22:6n3*. *J Lipid Res*, 2012. **53**(3): p. 494-504.
151. Quehenberger, O., et al., *Lipidomics reveals a remarkable diversity of lipids in human plasma*. *J Lipid Res*, 2010. **51**(11): p. 3299-305.
152. Livak, K.J. and T.D. Schmittgen, *Analysis of relative gene expression data using real-time quantitative PCR and the 2(-Delta Delta C(T)) Method*. *Methods*, 2001. **25**(4): p. 402-8.

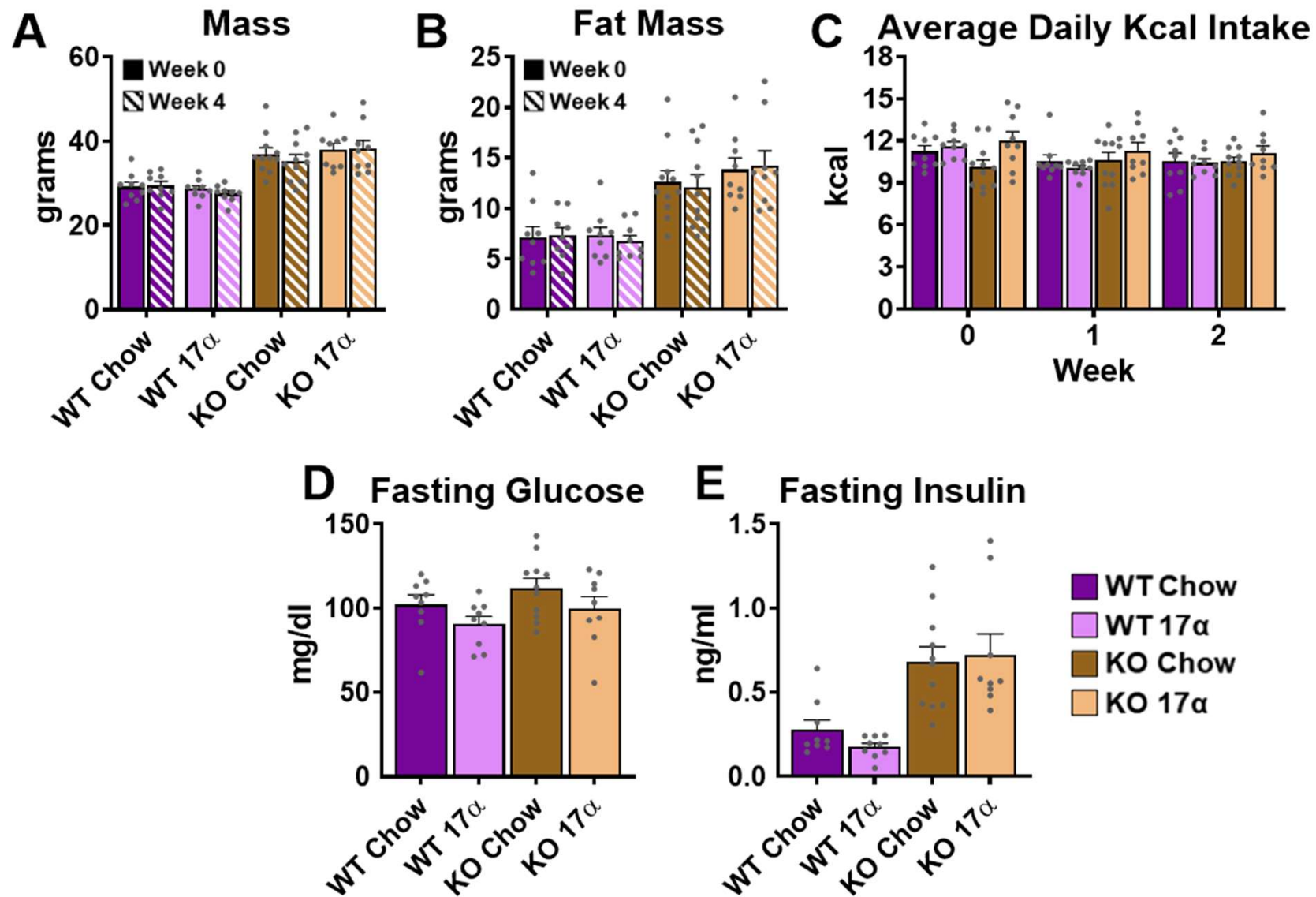


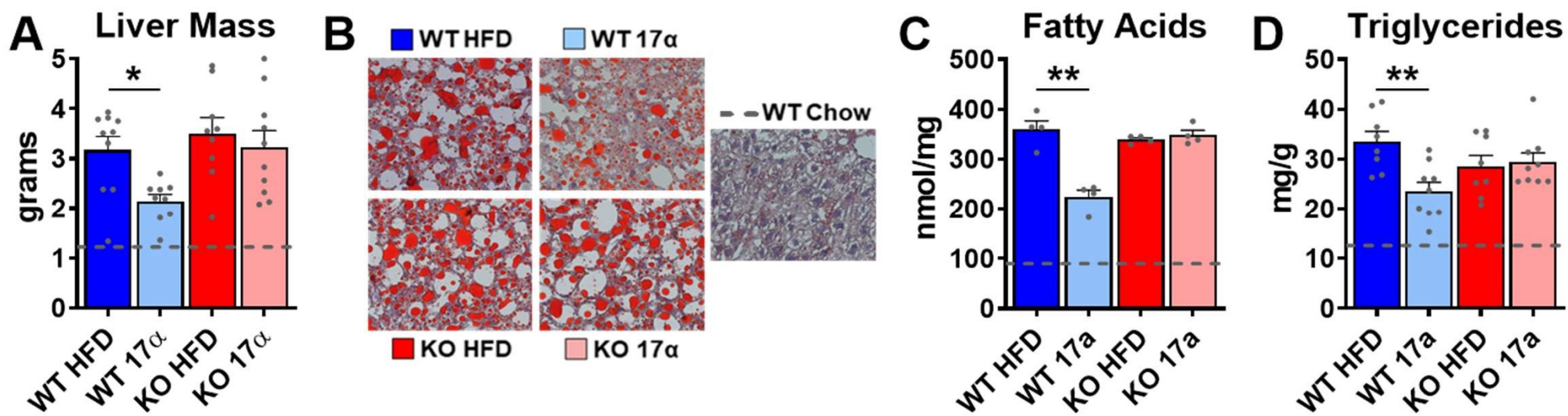


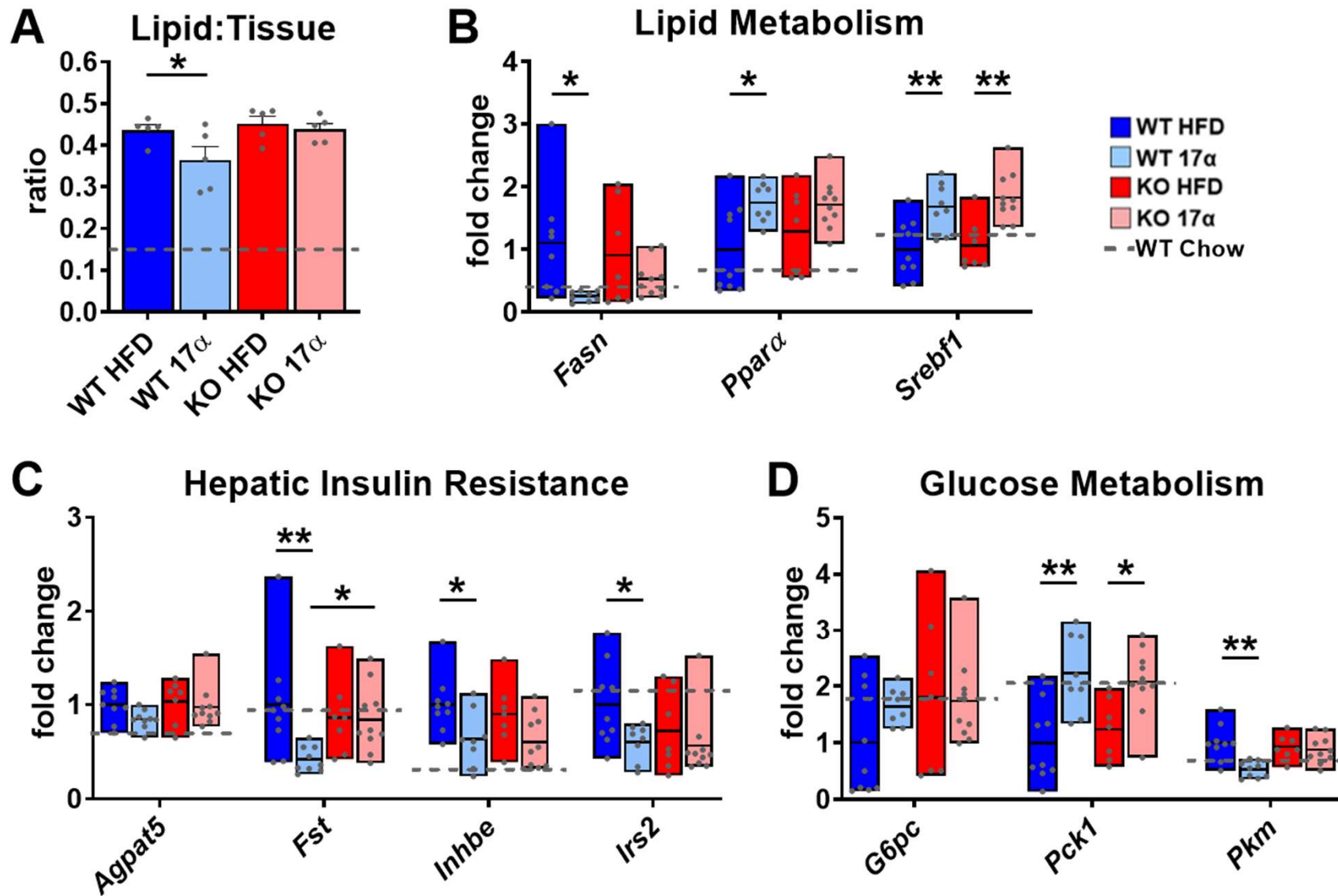












Liver Fatty Acid Profile

